

Journal article

Shengqian Chen*, Andrew J. Majda, and Samuel N. Stechmann

Multiscale asymptotics for the Skeleton of the Madden-Julian Oscillation and Tropical–Extratropical Interactions

Abstract: A new model is derived and analyzed for tropical–extratropical interactions involving the Madden–Julian oscillation (MJO). The model combines (i) the tropical dynamics of the MJO and equatorial baroclinic waves and (ii) the dynamics of barotropic Rossby waves with significant extratropical structure, and the combined system has a conserved energy. The method of multiscale asymptotics is applied to systematically derive a system of ordinary differential equations (ODEs) for three-wave resonant interactions. Two novel features are (i) a degenerate auxiliary problem with overdetermined equations due to a compatibility condition (meridional geostrophic balance) and (ii) cubic self-interaction terms that are not typically found in three-wave resonance ODEs. Several examples illustrate applications to MJO initiation and termination, including cases of (i) the MJO, equatorial baroclinic Rossby waves, and barotropic Rossby waves interacting, and (ii) the MJO, baroclinic Kelvin waves, and barotropic Rossby waves interacting. Resonance with the Kelvin wave is not possible in a dry model, but it occurs in the moist model here through interactions with water vapor and convective activity.

Keywords: tropical intraseasonal variability, tropical-extratropical interactions, multiscale asymptotic analysis

PACS: 02.30.Mv, 92.60.Ox

Received This draft: June 11, 2015

***Corresponding Author: Shengqian Chen:** Department of Mathematics, University of Wisconsin – Madison, Madison, Wisconsin, USA, sqchen@math.wisc.edu

Andrew J. Majda: Department of Mathematics, and Center for Atmosphere-Ocean Sciences, Courant Institute of Mathematical Science, New York University, New York, New York, USA, jonjon@cims.nyu.edu

Samuel N. Stechmann: Department of Mathematics, and Department of Atmospheric and Oceanic Sciences, University of Wisconsin – Madison, Madison, Wisconsin, USA, stechmann@wisc.edu

1 Introduction

The Madden-Julian Oscillation (MJO) is the dominant component of intraseasonal (≈ 30 -60 days) variability in the tropics [7, 8, 9]. It is an equatorial wave envelope of complex multi-scale convective processes, coupled with planetary-scale ($\approx 10,000$ -40,000 km) circulation anomalies. Individual MJO events propagate eastward at a speed of roughly 5 m/s, and their convective signal is most prominent over the Indian and western Pacific Oceans [33]. In addition to its significance to its own right, the MJO also significantly affects many other components of the atmosphere-ocean-earth system, such as monsoon development, intraseasonal predictability in mid-latitude, and the development of the El Niño southern oscillation (ENSO) [6, 33].

In addition to its strong tropical signal, the MJO interacts with the global flow on the intraseasonal timescales. Teleconnection patterns between the global extratropics and the MJO were described in an early observational analysis by Weickmann (1983) [30] and Weickmann *et al.* (1985) [32]. Their results demonstrate coherent fluctuations between extratropical flow and eastward-propagating outgoing longwave radiation (OLR) anomalies in the tropics. In the study by Matthews and Kiladis (1999) [17], they illustrate the interplay between high-frequency transient extratropical waves and the MJO. More recently, Weickmann and Berry (2009) [31] demonstrate that convection in the MJO frequently evolves together with a portion of the activity in a global wind oscillation.

The interactions between extratropical waves and tropical convection have also been investigated in numerical models. To view the extratropical response to convective heating, Jin and Hoskins (1995) [3] forced a primitive equation model with a fixed heat source in the tropics in the presence of a climatological background flow and obtain the Rossby wave train response in the result. To diagnose the more specific response to patterns of convection more like those of the observed MJO, Matthews *et al.* (2004)[16] forced a primitive equation model in a climatological background flow with patterns of observed MJO. The resulting global response to that heating is similar in many respects to the observational analysis. The MJO initiation in response to extratropical waves was illustrated by Ray and Zhang (2010) [20]. They show that a dry-channel model of the tropical atmosphere developed MJO-like signals in tropical wind fields when forced by reanalysis fields at poleward boundaries.

How can one model the two-way interaction between MJO and extratropical waves in a simplified, integrative way? This is the primary question of the present paper. Section 2 introduces a planetary scale model for this purpose. The

model includes (i) barotropic dynamics that span the tropics and extratropics, (ii) equatorial baroclinic dynamics, and (iii) the interactive effects of moisture and convection. More specifically, the model integrates the dry barotropic–first baroclinic interaction that has been studied by Majda and Biello (2003) [11] and Khouider and Majda (2005)[4] with the MJO skeleton model first developed by Majda and Stechmann (2009) [14] and further investigated by same authors [15]. In these previous studies, Majda and Biello (2003) carry out a multiscale asymptotic analysis for the resonant interactions of dry baroclinic Rossby waves and barotropic Rossby waves; and the MJO skeleton model [14] has captured three main features of the MJO on planetary/intraseasonal scales: (i) slow eastward phase speed of roughly 5m/s; (ii) peculiar dispersion relation with $d\omega/dk \approx 0$; (iii) horizontal quadrupole vortex structure.

A multiscale asymptotic analysis is presented here in Section 3 and later sections, adopting similar strategies as in Majda and Biello (2003), based on long-wave scales, small amplitude assumption, and multiple long time scales. The long-wave scaling leads to meridional geostrophic balance at the leading order, which appears as a constraint in the partial differential equation (PDE) system. This constraint complicates the auxiliary problem of the multiscale analysis, which is described and resolved in Section 4 and is a necessary step for suppressing secular terms. Section 5 presents the dispersion relation of the leading order linear operator for both the baroclinic and barotropic modes. In Section 6, by inspecting the dispersion curves of the linear operator, three-wave resonant interactions are identified, and an ODE system for wave interactions is derived using multiscale asymptotics. A novel feature of this ODE system is the presence of cubic self-interactions terms, which are not typically found in three-wave interaction ODEs (e.g., [1, 10, 19, 21, 22]). Here the cubic self-interaction arises from the new nonlinearity in the MJO skeleton model involving water vapor and convective activity.

Readers who are most interested in physical applications can skip ahead to Section 6, where the reduced ODE model is presented. The results with the model are then organized as follows. First, in Section 7, a validation study is presented to explore the time scales of validity of the asymptotic model. Second, in Section 8, numerical simulations are presented for three-wave interactions. Two cases of three-wave interactions are chosen for application to MJO initiation and termination [20, 23] and tropical–extratropical interaction. Each case therefore involves both the MJO and barotropic Rossby waves, and the third wave is either a dry baroclinic Rossby wave or a dry Kelvin wave. Interactions involving the Kelvin wave have not previously been emphasized in earlier work, and in a dry model [11] they are not possible. Here the resonant interaction

of the baroclinic Kelvin wave and barotropic Rossby wave is made possible by using a model with water vapor and convective activity.

The details of the multiscale asymptotic analysis are presented in the appendices. In Appendix A and B, a meridional truncated system is formulated. Appendix C provides the explicit formulation of the auxiliary problems. Finally, the details of the derivation of the reduced ODE system are given in Appendix D.

2 The two-layer equatorial β -plane equations

The nondimensional two-layer equatorial β -plane equations for the barotropic and baroclinic MJO skeleton model are given by

$$\frac{\partial \bar{\mathbf{v}}}{\partial t} + \bar{\mathbf{v}} \cdot \nabla \bar{\mathbf{v}} + y \bar{\mathbf{v}}^\perp + \nabla \bar{p} = -\frac{1}{2} \nabla \cdot (\mathbf{v} \otimes \mathbf{v}), \quad (1a)$$

$$\nabla \cdot \bar{\mathbf{v}} = 0, \quad (1b)$$

$$\frac{\partial \mathbf{v}}{\partial t} + \bar{\mathbf{v}} \cdot \nabla \mathbf{v} - \nabla \theta + y \mathbf{v}^\perp = -\mathbf{v} \cdot \nabla \bar{\mathbf{v}}, \quad (1c)$$

$$\frac{\partial \theta}{\partial t} + \bar{\mathbf{v}} \cdot \nabla \theta - \nabla \cdot \mathbf{v} = \delta^2 (\bar{H}a - S^\theta), \quad (1d)$$

$$\frac{\partial q}{\partial t} + \bar{\mathbf{v}} \cdot \nabla q + \tilde{Q} \nabla \cdot \mathbf{v} = -\delta^2 (\bar{H}a - S^q), \quad (1e)$$

$$\frac{\partial a}{\partial t} = \Gamma q a. \quad (1f)$$

These equations combine the MJO skeleton model [14] and nonlinear interactions between the baroclinic and barotropic modes [11]. The equations have been nondimensionalized using the scales listed in Table 1. Here $\bar{\mathbf{v}} = (\bar{u}, \bar{v})$ and \bar{p} are barotropic velocity and pressure; $\mathbf{v} = (u, v)$ and θ are baroclinic velocity and potential temperature; and q is water vapor (sometimes referred to as “moisture”). The tropical convective activity envelope is denoted by $\delta^2 a$, where δ is a small parameter that monitors the scales of tropical convection envelope. Likewise, δ^2 is also applied to quantities S^θ and S^q , radiative cooling and the moisture source. In this paper, $\delta^2 S^\theta$ and $\delta^2 S^q$ are set to be constants for energy conservation, although they usually have both spatial and temporal variance in reality. Together with Γ , \bar{H} and \tilde{Q} , the coefficients are described in table 2.

In equations (1), $\mathbf{v}^\perp = (-v, u)$ is the β -plane approximation of tropical Coriolis force, and (x, y) denotes the zonal and meridional directions. Without the moisture q and convection envelope a , system (1) is the two-vertical-mode Galerkin truncation for the Boussinesq equations with rigid-lid boundary on the

Par.	Derivation	Dim. val.	Description
β		$2.3 \times 10^{-11} \text{ m}^{-1} \text{ s}^{-1}$	Variation of Coriolis parameter with latitude
θ_0		300 K	Potential temperature at surface
g		9.8 m s^{-2}	Gravitational acceleration
H		16 km	Tropopause height
N^2	$(g/\theta_0)d\bar{\theta}/dz$	10^{-4} s^{-2}	Buoyancy frequency squared
c	NH/π	50 m s^{-1}	Velocity scale
X_e	$\sqrt{c/\beta}$	1500 km	Equatorial length scale
T	X_e/c	8 hrs	Equatorial time scale
	$HN^2\theta_0/(\pi g)$	15 K	Potential temperature scale
	H/π	5 km	Vertical length scale
	$H/(\pi T)$	0.2 m s^{-1}	Vertical velocity scale
	c^2	$2500 \text{ m}^2 \text{ s}^{-2}$	Pressure scale

Table 1. Constants and reference scales for nondimensionalization.

Par.	Non-dim. val.	Dim. val.	Description
Γ	1	$\sim 0.5 \text{ /day}/(\text{g/kg})$	Convective growth/decay rate
\bar{H}	0.23	$\sim 10 \text{ K/day}$	Parameter to rescale a
$\delta^2 \bar{a}$	δ^2		Convective activity envelope at RCE state
\tilde{Q}	0.9		Non-dim. background vertical moisture gradient
$\delta^2 S^\theta$	$\delta^2 \bar{H}$		Radiative cooling rate
$\delta^2 S^q$	$\delta^2 \bar{H}$		Moisture source

Table 2. Parameters of the MJO skeleton model, and relation to small parameter δ .

vertical direction (see e.g., [18, 12, 11, 4]) Without the barotropic wind $\bar{\mathbf{v}}$, the system is the MJO skeleton model on the first baroclinic mode (see e.g., [14, 15]).

Note that for the primitive equations (1), a total energy is conserved, and it is composed of four parts, dry barotropic energy \mathcal{E}_T , dry baroclinic energy \mathcal{E}_C , moisture energy \mathcal{E}_M , and convective energy \mathcal{E}_A :

$$\mathcal{E}_T(t) = \frac{1}{2} \int_{-Y}^Y \int_0^X |\bar{\mathbf{v}}|^2 dx dy \quad (2a)$$

$$\mathcal{E}_C(t) = \frac{1}{4} \int_{-Y}^Y \int_0^X |\mathbf{v}|^2 + \theta^2 dx dy \quad (2b)$$

$$\mathcal{E}_M(t) = \frac{1}{4} \int_{-Y}^Y \int_0^X \frac{1}{\bar{Q}(1-\bar{Q})} (q + \bar{Q}\theta)^2 dx dy \quad (2c)$$

$$\mathcal{E}_A(t) = \frac{\delta^2}{2} \int_{-Y}^Y \int_0^X \frac{1}{\bar{Q}\Gamma} [\bar{H}a - S^\theta \log(a)] dx dy \quad (2d)$$

This energy conservation forms the design principle as appeared in [14, 11]. Note that in (1f), the conserved quantity \mathcal{E} still holds if a is also advected by the barotropic wind, i.e., with an additional term $\bar{\mathbf{u}} \cdot \nabla a$ in (1f). But we do not include this term because later, when meridional truncation is applied to the system, the energy conservation will not hold with this additional term.

Using the streamfunction ψ for barotropic mode, which satisfies $(\bar{\mathbf{u}}, \bar{\mathbf{v}}) = (-\psi_y, \psi_x)$, the barotropic equation can also be written as

$$\frac{D}{Dt} \Delta \psi + \psi_x + \frac{1}{2} \nabla \cdot [-(\mathbf{v}u)_y + (\mathbf{v}v)_x] = 0, \quad (3)$$

where

$$\frac{D}{Dt} = \frac{\partial}{\partial t} + \bar{u} \frac{\partial}{\partial x} + \bar{v} \frac{\partial}{\partial y}$$

represents advection by the barotropic wind.

2.1 The zonal-long wave scaled model

To consider the planetary scale of the coupled equations in (3) and (1c)-(1f), zonal variations are assumed to depend on a longer scale, as are temporal variations. The long zonal and long temporal coordinates are introduced as

$$x' = \delta x, \quad t' = \delta t. \quad (4)$$

Correspondingly, the meridional velocity is also scaled so that

$$v = \delta v'. \quad (5)$$

The equations in (3) and (1c)-(1f) become the long-wave-scaled system:

$$\frac{D}{Dt'} \psi_{yy} + \psi_{x'} - \frac{1}{2} \nabla' \cdot [(\mathbf{v}'u)_y] + \delta^2 \left\{ \frac{D}{Dt'} \psi_{x'x'} + \frac{1}{2} \nabla' \cdot [(\mathbf{v}'v')_{x'}] \right\} = 0, \quad (6a)$$

$$\frac{D}{Dt'} u - \theta_x - yu - \mathbf{v}' \cdot \nabla' \psi_y = 0, \quad (6b)$$

$$-\theta_y + yu + \delta^2 \left(\frac{D}{Dt'} v' + v' \cdot \nabla' \psi_{x'} \right) = 0 \quad (6c)$$

$$\frac{D}{Dt'} \theta - \nabla' \cdot \mathbf{v}' - \delta(\bar{H}a - S^\theta) = 0, \quad (6d)$$

$$\frac{D}{Dt'} q + \tilde{Q} \nabla' \cdot \mathbf{v}' + \delta(\bar{H}a - S^q) = 0, \quad (6e)$$

$$\frac{\partial}{\partial t'} a - \Gamma q a = 0. \quad (6f)$$

Here the primes represent the long-wave scaled coordinates and variables:

$$\frac{D}{Dt'} = \frac{\partial}{\partial t'} + u \frac{\partial}{\partial x'} + v' \frac{\partial}{\partial y'}, \quad \nabla' = \left(\frac{\partial}{\partial x'}, \frac{\partial}{\partial y'} \right), \quad \text{and} \quad \bar{\mathbf{v}}' = (u, v').$$

System (6) is in the same form as in [11] when the moisture and convection are neglected.

Furthermore, the convective activity a will be written as an anomaly from the state of radiative-convective equilibrium (RCE):

$$S^\theta = S^q = \bar{H}\bar{a},$$

where these constants take the values given in table 2. When $a = \bar{a}$, the external radiative cooling/moisture source is in balance with the source/sink from the convection, and the system achieves RCE. By writing a as an anomaly with respect to the RCE value \bar{a} , the forcing terms in (6d) and (6e) can be written as

$$\bar{H}a - S^\theta = \bar{H}a - S^q = \bar{H}(a - \bar{a}) = \bar{H}a', \quad (7)$$

and the equation for the convection envelope (6f) can be written as

$$\frac{\partial}{\partial t'} a' - \Gamma \bar{a} q = \Gamma a' q. \quad (8)$$

2.2 Long time scales for tropical–extratropical interactions

The small parameter δ is also used for introducing two longer time scales:

$$T_1 = \delta t', \quad T_2 = \delta^2 t'.$$

Their units match the units of intraseasonal timescales as appeared in [11, 13].

In the next section, the system is expanded by matching the orders of δ .

3 Asymptotic expansions for the interaction of barotropic and equatorial baroclinic waves

In this section, asymptotic expansions are carried out twice: first for the 2-D system as functions of x and y , and second for a system using a truncated basis for variations in the y direction. The first expansion (2-D) provides the clearest presentation, but the 2-D linear operator does not have eigenvalues and eigenfunctions that are easily accessible. For this reason, the second, truncated system is introduced and provides a linear operator with known eigenvalues and eigenfunctions.

3.1 The 2-D equations

Assume that the solutions have an asymptotic structure with **ansatz**:

$$(\psi, u, v', \theta, q) = \delta^2(\psi_1, u_1, v_1, \theta_1, q_1) + \delta^3(\psi_2, u_2, v_2, \theta_2, q_2) + \delta^4(\psi_3, u_3, v_3, \theta_3, q_3) + o(\delta^4) \quad (9a)$$

$$\text{and} \quad a' = \delta a_1 + \delta^2 a_2 + \delta^3 a_3 + O(\delta^4), \quad (9b)$$

This small amplitude assumption is consistent with a small Froude number assumption as in [11]. All variables are assumed to depend on three time scales: t' and $T_1 = \delta t'$ and $T_2 = \delta^2 t'$. The system is expanded over three orders of magnitude.

The **first order system** is

$$\psi_{1y'y't'} + \psi_{1x'} = 0, \quad (10a)$$

$$u_{1t'} - \theta_{1x'} - y'v_1 = 0, \quad (10b)$$

$$- \theta_{1y'} + y'u_1 = 0, \quad (10c)$$

$$\theta_{1t'} - u_{1x'} - v_{1y'} - \bar{H}a_1 = 0, \quad (10d)$$

$$q_{1t'} + \tilde{Q}(u_{1x'} + v_{1y'}) + \bar{H}a_1 = 0, \quad (10e)$$

$$a_{1t'} - \Gamma\bar{a}q_1 = 0. \quad (10f)$$

This system defines the leading-order linear operator, including a combination of barotropic Rossby waves [11] from the dynamics of ψ and baroclinic equatorial long-waves including the MJO [14] from the other variables.

The **second order system** is

$$\psi_{2y'y't'} + \psi_{2x'} = -\psi_{1y'y'T_1}, \quad (11a)$$

$$u_{2t'} - \theta_{2x'} - y'v_2 = -u_{1T_1}, \quad (11b)$$

$$- \theta_{2y'} + y'u_2 = 0, \quad (11c)$$

$$\theta_{2t'} - u_{2x'} - v_{2y'} - \bar{H}a_2 = -\theta_{1T_1}, \quad (11d)$$

$$q_{2t'} + \tilde{Q}(u_{2x'} + v_{2y'}) + \bar{H}a_2 = -q_{1T_1}, \quad (11e)$$

$$a_{2t'} - \Gamma\bar{a}q_2 = -a_{1T_1} + \Gamma a_1 q_1. \quad (11f)$$

Note that the only nonlinear term is from the q - a interaction: $\Gamma a_1 q_1$.

The **third order system** is

$$\begin{aligned} \psi_{3y'y't'} + \psi_{3x'} = & -\psi_{1y'y'T_2} - \psi_{2y'y'T_1} \\ & - \left[\psi_{1x'x't'} + \psi_{1x'}\psi_{1y'y'y'} - \psi_{1y'}\psi_{1x'y'y'} - \frac{1}{2}(u_1^2)_{x'y'} - \frac{1}{2}(u_1v_1)_{y'y'} \right], \end{aligned} \quad (12a)$$

$$u_{3t'} - \theta_{3x'} - y'v_3 = -u_{1T_2} - u_{2T_1} - [\psi_{1x'}u_{1y'} - \psi_{1y'}u_{1x'} - u_1\psi_{1x'y'} - v_1\psi_{1y'y'}], \quad (12b)$$

$$- \theta_{3y'} + y'u_3 = -v_{1t'}, \quad (12c)$$

$$\theta_{3t'} - u_{3x'} - v_{3y'} - \bar{H}a_3 = -\theta_{1T_2} - \theta_{2T_1} - \psi_{1x'}\theta_{1y'} + \psi_{1y'}\theta_{1x'}, \quad (12d)$$

$$q_{3t'} + \tilde{Q}(u_{3x'} + v_{3y'}) + \bar{H}a_3 = -q_{1T_2} - q_{2T_1} - \psi_{1x'}q_{1y'} + \psi_{1y'}q_{1x'}, \quad (12e)$$

$$a_{3t'} - \Gamma\bar{a}q_3 = -a_{1T_2} - a_{2T_1} + \Gamma(a_1q_2 + a_2q_1) - \psi_{1x'}a_{1y'} + \psi_{1y'}a_{1x'}. \quad (12f)$$

Note that more nonlinear terms arise, including the baroclinic–barotropic interactions as in [11].

With the assumption in (9), the total energy is approximately conserved:

$$\frac{d}{dt'}\mathcal{E} = o(\delta^4). \quad (13)$$

MJO skeleton model	Dry wave model in [11]
Moisture equations involving q and a are included	Dry dynamics only
Small parameter δ	Small parameter $\epsilon = \delta^2$
$\delta = \sqrt{0.1}$, $\epsilon = 0.1$	
Two long time scales: $T_1 = \delta t'$ and $T_2 = \delta^2 t'$	One long time scale: $\tau = \epsilon t'$
$T_1 = O(3 \text{ day})$, $T_2 = O(10 \text{ day})$	
Linear system is dispersive	Linear system is non-dispersive

Table 3. Comparisons between the MJO model here and the dry wave model of [11].

from the asymptotic expansions (10)-(12). This approximated energy conservation is important to preserve in future derivations.

The asymptotic expansions (10)-(12) are analogous to the expansions in [11], where the system did not have moisture q nor convection envelope a . Nonetheless, there are essential differences described in table 3. For example, in [11], the small parameter was $\epsilon = \delta^2$, in which case the ansatz in (9) includes only the δ^2 and δ^4 terms, and only the systems in (10) and (12) arise. On the other hand, here the small parameter is δ , which leads to the additional δ^3 terms in the ansatz (9) and the additional system in (11).

Unfortunately, the 2-D linear operator defined in (10) does not have eigenvalues and eigenfunctions that are easily accessible. This is due to the effects of moisture q and convective activity a , since on the other hand the “dry” dynamics without q and a do have well-known eigenvalues and eigenfunctions [11]. Since the method of multiscale asymptotics relies heavily on the leading order linear operator, further progress cannot be made with the systems (10)–(12).

To circumvent this issue, a truncated basis will be introduced next in section 3.2 for variations in the y direction, and the truncated system has eigenvalues and eigenvectors that have previously been presented [14]. The truncated system utilizes Riemann invariants $l = -(u + \theta)/\sqrt{2}$ and $r = (u - \theta)/\sqrt{2}$ [10] in place of the variables u and θ .

3.2 Meridional truncated system

To simplify the system, a meridional truncation is adopted as in the truncations in MJO skeleton model [14] by using parabolic cylinder functions for baroclinic variables. The barotropic variables are assumed to be sinusoidal as in [11]. Although mostly similar to [14] and [11], some modifications are needed for energy conservation, as described further below. Explicitly, the **meridional trunca-**

tion is

$$\psi = B(x, t) \sin(Ly) \quad (14a)$$

$$(l, r, q) = \left(l^{(0)}(x, t), r^{(0)}(x, t), q^{(0)}(x, t) \right) \Phi_0(y), \quad (14b)$$

$$+ \left(l^{(2)}(x, t), r^{(2)}(x, t), q^{(2)}(x, t) \right) \Phi_2(y), \quad (14c)$$

$$v' = v^{(1)} \Phi_1(y), \quad (14d)$$

$$a' = a^{(0)}(x, t) \Phi_0(y), \quad (14e)$$

where $\Phi_m(y)$ are parabolic cylinder functions:

$$\Phi_m(y) = (m! \sqrt{\pi})^{-\frac{1}{2}} 2^{-\frac{m}{2}} e^{-\frac{y^2}{2}} H_m(y), \quad (15)$$

with Hermite polynomials $H_m(y)$ defined by

$$H_m(y) = (-1)^m e^{y^2} \frac{d^m e^{-y^2}}{dy^m}. \quad (16)$$

The parabolic cylinder functions form an orthonormal basis on the 1D function space. The first few functions are

$$\Phi_0(y) = \pi^{-\frac{1}{4}} e^{-y^2/2}, \quad \Phi_1(y) = \pi^{-\frac{1}{4}} \sqrt{2} y e^{-y^2/2}, \quad \Phi_2(y) = \pi^{-\frac{1}{4}} \frac{1}{\sqrt{2}} (2y^2 - 1) e^{-y^2/2}. \quad (17)$$

The parabolic cylinder functions satisfy the following identities:

$$L_+ \Phi_m(y) = (2m)^{1/2} \Phi_{m-1}(y), \quad L_- \Phi_m(y) = -[2(m+1)]^{1/2} \Phi_{m+1}(y), \quad (18)$$

which help to simplify the expression, where the operators L_\pm are defined as

$$L_\pm = \frac{\partial}{\partial y} \pm y.$$

In the truncation (14a), the parameter

$$L = \frac{2\pi}{2Y}$$

is the meridional wavenumber, and $2Y$ is the meridional wavelength.

Applying this meridional truncation to the 2-D model in (6) leads to the **truncated system**:

$$L^2 Y B_{t'} - Y B_{x'} = \mathcal{C}_T + \delta^2 (Y B_{x'x't'} + \mathcal{D}_T), \quad (19a)$$

$$\mathcal{N} \vec{U}_t + \mathcal{L} \vec{U} = \vec{C}_C + \delta^2 \vec{D}_C, \quad (19b)$$

where $\vec{U} = (l^{(0)}, l^{(2)}, r^{(0)}, r^{(2)}, v^{(1)'}, q^{(0)}, q^{(2)}, a^{(0)})$, $\mathcal{L}_{\vec{U}}$ is the spatial linear operator, and $\mathcal{N} = \text{diag}(1, 1, 1, 1, 0, 1, 1, 1)$ is an 8×8 diagonal matrix with the 0 placed in the $v^{(1)'}$ element of the diagonal. At the right hand side, \mathcal{C}_T , \mathcal{D}_T , $\vec{\mathcal{C}}_C$ and $\vec{\mathcal{D}}_C$ are bilinear terms at different orders in the long-wave scaled system. These bilinear terms are from advection terms in the 2-D system (i.e., $\bar{\mathbf{v}} \cdot \nabla \bar{\mathbf{v}}$, $\nabla \cdot (\mathbf{v} \otimes \mathbf{v})$, $\bar{\mathbf{v}} \cdot \nabla \mathbf{v}$, $\mathbf{v} \cdot \nabla \bar{\mathbf{v}}$) and nonlinear q - a interaction: $\Gamma q a$. The detailed expressions are given in (36) in Appendix A.

This particular meridional truncation (14) is used because it maintains the $l^{(0)}$ - $v^{(1)}$ - $r^{(2)}$ triplets to obtain the correct dispersion relation for baroclinic Rossby waves [10]. Also, this meridional truncation imitates the energy conservation as in the full system with minimal alteration in the $a^{(0)}$ equation. Other truncations may also be considered, such as neglecting $l^{(2)}$ and $q^{(2)}$ as in MJO skeleton model [14], and we have explored several other options. However, other truncations can potentially contribute to energy imbalance from the barotropic advection acting on baroclinic variables.

Finally, the truncated system (19) can be expanded in powers of δ , similar to the expansion (10)–(12) of the 2-D system (6). The expansion of (19) is presented in Appendix B in (42)–(44). The next step in the method of multiscale asymptotics is to solve the auxiliary problem that arises in each of (42), (43), and (44).

4 Auxiliary problem: a degenerate system with constraint equation

In this section, the auxiliary problem is introduced. It is a key part of the multi-scale analysis procedure where a forced linear system must be solved (see chapter 5 of [10] for other examples). In the linear system of the present paper, a difficulty arises because of a constraint equation; specifically, a constraint arises from meridional geostrophic balance where $v^{(1)}_{1t}$ does not appear in the leading order linear operator in (10) or (36). This constraint equation presents a difficulty for directly computing the eigenmodes of the linear system. To overcome this difficulty, a reformulation of the auxiliary problem is presented here to enable direct calculation of the eigenmodes and hence a direct solution of the forced linear system.

The linear system in \vec{U} for the baroclinic component from (19) can be denoted as:

$$\mathcal{N}\vec{U}_t + \mathcal{L}_{\vec{U}}\vec{U} = \vec{F}_{\vec{U}}. \quad (20)$$

Notice the degenerate diagonal 8×8 matrix $\mathcal{N} = \text{diag}(1, 1, 1, 1, 0, 1, 1, 1)$, which is degenerate due to the 0 in the $v^{(1)'}$ element of the diagonal. Here $\vec{F}_{\vec{U}}$ is the forcing term, including long-time dependency and bilinear terms. Also recall from (19) that \vec{U} is the vector of baroclinic variables, defined as $\vec{U} = (l^{(0)}, l^{(2)}, r^{(0)}, r^{(2)}, v^{(1)'}, q^{(0)}, q^{(2)}, a^{(0)})$. Due to the degenerate matrix \mathcal{N} , the eigenmodes of this system cannot be found directly using the standard procedure.

In order to circumvent the degenerate matrix \mathcal{N} , the auxiliary problem can be reformulated in terms of new variables:

$$\vec{W} = (K, R, Q, A, v^{(1)}, \chi, l^{(2)}, q^{(2)}),$$

where $K = r^{(0)}$, $R = \sqrt{2}l^{(0)} + 2r^{(2)}$, $Q = q^{(0)}$, $A = a^{(0)}$, $\chi = l^{(0)} - \sqrt{2}r^{(2)}$. This reversible linear transformation can be written as $\vec{W} = \mathcal{A}\vec{U}$. Then the system for \vec{W} is

$$\mathcal{A}\mathcal{N}\mathcal{A}^{-1}\partial_t\vec{W} + \mathcal{A}\mathcal{L}_{\vec{U}}\mathcal{A}^{-1}\vec{W} = \mathcal{A}\vec{F}_{\vec{U}}, \quad (21)$$

which can be further simplified to

$$\partial_t\vec{W} + \mathcal{L}_{\vec{W}}\vec{W} = \vec{F}_{\vec{W}}, \quad (22)$$

where $\vec{W} = (K, R, Q, A, l^{(2)}, q^{(2)})$, and $\mathcal{L}_{\vec{W}}$ is the spatial linear operators. From \vec{W} to \vec{W} , two variables $v^{(1)}$ and χ are eliminated because of the constraint equation. For details, see Appendix C.

Note that this transformation of variables from \vec{U} to \vec{W} is used in the formulation of the MJO skeleton model [14, 24], and it has some similarities to the transformation of the two-dimensional incompressible fluid flow equations from velocity variables to vorticity/streamfunction variables (see chapter 9 of [10]). For the purposes here, the formulation in terms of $\vec{W} = (K, R, Q, A, l^{(2)}, q^{(2)})$ allows easy identification of the linear eigenmodes of the linear operator $\mathcal{L}_{\vec{W}}$, since the (K, R, Q, A) sub-system of (22) is the linearized MJO skeleton model that has been previously studied [14].

Finally, the forcing $\vec{F}_{\vec{U}}$ in (20) must be transformed into $\vec{F}_{\vec{W}}$ in (22). This transformation is needed in order to solve the auxiliary problem at each order of magnitude in the asymptotic expansion. See Appendix C for the explicit formulas for $\vec{F}_{\vec{W}}$ for each order of magnitude of the asymptotic expansion.

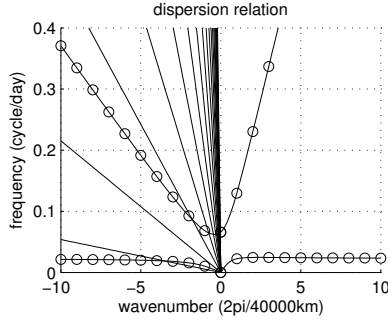


Fig. 1. Dispersion relation of the KRQA system (with circles) and barotropic wind with different meridional wavelengths (without circles).

5 Eigenmodes for the linear system

In this section, the eigenmodes are described for the baroclinic system and barotropic system. (Later, in Section 6, these linear eigenmodes will be used in the identification of three-wave resonances.)

First, in the baroclinic system (22) (with $\vec{F}_{\vec{W}} = \vec{0}$), the components of vector $\vec{W} = (K, R, Q, A, l^{(2)}, q^{(2)})$ can be separated into two groups: (K, R, Q, A) and $(l^{(2)}, q^{(2)})$. The KRQA system is closed (as can be seen in its explicit formulation in Appendix C), and its four eigenmodes have been described previously [14]: dry Kelvin, MJO, moist Rossby and dry Rossby, as shown in figure 1. In brief, the dry Kelvin wave is a fast eastward-propagating wave; the MJO is a slow east-propagating wave; and the moist and dry baroclinic Rossby waves are slow and fast westward-propagating waves, respectively. In addition to the KRQA system, $l^{(2)}$ satisfies an independent (decoupled) equation, and $q^{(2)}$ is slaved to (K, R, Q, A) and $l^{(2)}$ (see the explicit formulation in Appendix C). Therefore the eigenmodes from the KRQA system of [14] are not affected by the additional two variables $l^{(2)}$ and $q^{(2)}$. Notice that the baroclinic Rossby and Kelvin waves in this model are dry equatorial waves, not convectively coupled equatorial waves (CCEWs) [5]. The model here is a planetary-scale model that does not explicitly resolve CCEWs, which occur mainly on smaller, synoptic scales. Nevertheless, one would expect similar wave interactions to hold for CCEWs, due to the similar structures of dry and convectively coupled waves, if a model were used that resolved such synoptic-scale convectively coupled waves.

Second, for the barotropic system (19a), the dispersion relation is written explicitly as

$$\omega_T(k) = -\frac{k}{L^2}. \quad (23)$$

The above formula implies that barotropic Rossby waves travel faster for smaller meridional wavenumber L or, equivalently, longer meridional wavelength Y . In figure 1, barotropic dispersion relation are shown with different meridional wave numbers.

6 The reduced asymptotic models

In this section, the following reduced asymptotic model is derived and its basic features are described:

$$-\partial_{T_2}\beta + id_2\beta + id_3\alpha_{j_1}^*\alpha_{j_2}^* = 0, \quad (24a)$$

$$-\partial_{T_2}\alpha_{j_1} + id_4\alpha_{j_1}^2\alpha_{j_1}^* + id_5\alpha_{j_1} + id_6\beta^*\alpha_{j_2}^* = 0, \quad (24b)$$

$$-\partial_{T_2}\alpha_{j_2} + id_7\alpha_{j_2}^2\alpha_{j_2}^* + id_8\alpha_{j_2} + id_9\beta^*\alpha_{j_1}^* = 0, \quad (24c)$$

where the coefficients d_j are all real numbers. This is a system of ODEs for three-wave resonance, where β is the complex amplitude of the barotropic Rossby waves, and α_{j_1} and α_{j_2} are the complex amplitudes of two baroclinic waves. For the applications of importance here, one of the α s will correspond to the MJO, and this ODE system describes its interaction with the other waves, with an aim toward MJO initiation and termination.

In brief, the terms in (24) fall into three groups that are linked to different features in the full 2D model (1): the cubic terms are associated with the nonlinear q - a interactions; the linear terms come from dispersive terms; the quadratic terms rise from the nonlinear baroclinic-barotropic interactions. Here, in particular, the cubic self-interaction terms are a novel feature that are not typically found in three-wave resonance ODEs, and they arise here from the effects of water vapor q and convective activity a .

In the remainder of this section, two basic properties of the system are described – energy conservation and a family of fixed points – and the derivation is sketched, with details of the derivation shown in Appendix D.

6.1 Energy conservation

The ODE system (24) satisfies the following energy conservation principle:

$$\frac{\partial}{\partial T_2} (\beta\beta^* + \alpha_{j_1}\alpha_{j_1}^* + \alpha_{j_2}\alpha_{j_2}^*) = 0. \quad (25)$$

This conserved quantity is a consequence that all coefficients are pure imaginary, and in particular, that

$$d_3 + d_6 + d_9 = 0, \quad (26)$$

which is a key component for energy conservation in three-wave interaction equations [10].

6.2 Fixed points in ODE system

In addition to the trivial fixed point of (24) where $\beta = \alpha_{j_1} = \alpha_{j_2} = 0$, a family of nontrivial fixed points also exists:

$$|\alpha_{j_1}|^2 = \frac{d_2^2 d_5 d_7 + d_2 d_3 d_6 d_8}{d_3^2 d_6 d_9 - d_2^2 d_4 d_7} \quad (27a)$$

$$|\alpha_{j_2}|^2 = \frac{d_2^2 d_4 d_8 + d_2 d_3 d_9 d_5}{d_3^2 d_6 d_9 - d_2^2 d_4 d_7} \quad (27b)$$

$$\beta = -\frac{d_3}{d_2} \alpha_{j_1}^* \alpha_{j_2}^* \quad (27c)$$

As two examples, consider the parameter values of the MRB and MKB cases of Section 8. For MRB, the M stands for MJO, the R stands for equatorial Rossby wave, and the B stands for barotropic Rossby wave; and for MKB, the M and B are the same, and the K stands for equatorial Kelvin wave. For these cases, the nontrivial fixed points would have amplitudes

$$|\alpha_{j_1}| \approx 0.24, \quad |\alpha_{j_2}| \approx 0.20, \quad |\beta| \approx 0.0033 \text{ for case MRB,} \quad (28a)$$

$$|\alpha_{j_1}| \approx 2.4, \quad |\alpha_{j_2}| \approx 7.5, \quad |\beta| \approx 0.34 \text{ for case MKB.} \quad (28b)$$

respectively (although the simulations in Section 8 are not set up to illustrate the dynamics near these nontrivial fixed points).

In a linear stability analysis (not shown), the system (8) is neutrally stable when linearized around the trivial fixed point of $\vec{0}$. On the other hand, when linearized around the two examples of the nontrivial fixed points, the system is unstable. It would be interesting to further explore these cases and their physical interpretations in the future.

6.3 Derivation

The derivation of (24) starts by assuming a leading order barotropic component of the form

$$B_1 = \frac{1}{\sqrt{E_T}} \beta(T_1, T_2) e^{i\theta_T} + \text{C.C.}, \quad (29)$$

where $\theta_T = k_T x' + \omega_T t'$, and E_T is the barotropic energy unit

$$E_T = 2Y L^2,$$

and leading order baroclinic variables of the form

$$\vec{W}_1 = \alpha_{j_1} e^{i\theta_{j_1}} \vec{r}_{j_1} + \alpha_{j_2} e^{i\theta_{j_2}} \vec{r}_{j_2} + \text{C.C.}, \quad (30)$$

where $\theta_j = k_j x' + \omega_j t'$, and \vec{r} represents a right eigenvector of the linear system with components

$$\vec{r}_j = (\hat{K}_{1,j}, \hat{R}_{1,j}, \hat{Q}_{1,j}, \hat{A}_{1,j}, l^{(\hat{2})}_{1,j}, q^{(\hat{2})}_{1,j}), \quad j = j_1, j_2.$$

Here the arbitrary complex phase factor of each eigenvector is chosen so that $\hat{K}_{1,j}$ is a real number, and the eigenvectors \vec{r}_j are normalized with respect to the energy as

$$E_j = \vec{r}_j^\dagger \mathcal{H} \vec{r}_j = 1, \quad j = j_1, j_2, \quad (31)$$

where \mathcal{H} is the Hessian matrix of the conserved energy for the linear baroclinic system.

Next, two auxiliary problems must be solved, (51) and (52) of Appendix C, one for each of the two long time scales, $T_1 = \delta t'$ and $T_2 = \delta^2 t'$. The solution of the auxiliary problems is the key step in the method of multiscale asymptotics in order to suppress secular growth and guarantee a consistent asymptotic expansion of the variables [10]. As part of the second auxiliary problem, the three waves must satisfy the following resonance conditions:

$$k_{j_1} + k_{j_2} + k_T = 0, \quad (32a)$$

$$\omega_{j_1} + \omega_{j_2} + \omega_T = 0. \quad (32b)$$

Further details of derivation are presented in Appendix D.

7 Validation study: the wavenumber–2 MJO mode

In this section, a special case is considered in order to explore the time scales of validity of the ODE system in (24). If only a single baroclinic mode is considered,

without a barotropic mode, the ODE system in (24) becomes a single ODE:

$$-\partial_{T_2} \alpha_{j_1} + id_4 \alpha_{j_1}^2 \alpha_{j_1}^* + id_5 \alpha_{j_1} = 0. \quad (33)$$

The energy conservation of this single mode then takes the form

$$\frac{\partial}{\partial T_2} (\alpha_{j_1} \alpha_{j_1}^*) = 0. \quad (34)$$

This special case can then be compared against numerical solutions that have been presented previously elsewhere [15], which will be regarded as the ‘true’ solution here. The specific case chosen is Case U2 of [15], which has a wavenumber-2 MJO eigenmode as the initial condition for a nonlinear simulation.

A few technical details for consistency with [15] are the following. The coefficient c_1 in (36) is taken to be 1 for consistency with the equation $A_t = \Gamma Q A$ used in [15]. Also, since the model of [15] does not include the dispersive effects of $v^{(1)}$ (although it does include other dispersive effects), the coefficient d_5 in the ODE system (33) is set to 0. As in [15], here the computational domain is $[0, X]$, where $X = 40,000$ km in the circumference of Earth at the equator.

For the validation study, three different values of δ are chosen: $\delta = \sqrt{0.1}$, $\sqrt{0.1}/2$ and $\sqrt{0.1}/4$, corresponding to three different RCE states: $\delta^2 \bar{a} = 0.1$, 0.025 and 0.00625. The solutions are evolved out to times 100, 200, and 400 days respectively, matching the long wave assumption. Table 4 shows the relative error between the asymptotic solution and the ‘exact’ solution. The *relative* error decreases by a factor of 2 as δ is decreased by a factor of 2, indicating a *relative* error of $O(\delta)$, in line with an *absolute* error of $O(\delta^3)$ and a true solution with magnitude of $O(\delta^2)$. Figures 2 and 3 show comparisons between the asymptotic solutions and numerical (‘true’) solutions for $\delta = \sqrt{0.1}$ and $\sqrt{0.1}/2$ (with $\delta = \sqrt{0.1}/4$ not shown since it is indistinguishable from the ‘true’ solution). In Figure 2, the agreement is good out to 100 days, although some of the peaks in convective activity $\bar{H}A$ are not captured by the asymptotic solution. In Figure 3, the agreement is excellent out to 200 days.

As a further validity test of the asymptotic model, the same comparisons have been repeated (not shown) with the addition of the second order corrections. More specifically, whereas the asymptotic solution \bar{W}_{asym} in Table 4 was defined as $\bar{W}_{\text{asym}} = \delta^2 \bar{W}_1$, the comparisons have been repeated using $\bar{W}_{\text{asym}} = \delta^2 \bar{W}_1 + \delta^3 \bar{W}_2$, where the second order correction \bar{W}_2 is described in more detail in Appendix C and D. In these new tests, the values of Table 4 change to 0.2685, 0.0627, 0.0183. These values show a decrease in *relative* error of a factor of 4 as δ is decreased by a factor of 2, indicating a *relative* error of $O(\delta^2)$, in line with an *absolute* error of $O(\delta^4)$ and a true solution with magnitude of $O(\delta^2)$.

	$\delta^2 \bar{a} = \mathbf{0.1}$ at 100 day	$\delta^2 \bar{a} = \mathbf{0.025}$ at 200 day	$\delta^2 \bar{a} = \mathbf{0.00625}$ at 400 day
$\ \vec{W}_{\text{asym}} - \vec{W}_n\ / \ \vec{W}_n\ $	0.3890	0.1657	0.0770

Table 4. The relative difference between numerical solution \vec{W}_n (regarded as the ‘true’ solution here) and the asymptotic solution (\vec{W}_{asym}) whose amplitude $\alpha_{j_1}(T_2)$ is governed by the ODE (33). Three different values of δ are considered along with three different corresponding times.

In summary, the asymptotic solutions have significant accuracy on time scales of 100 days or longer, which are roughly the time scales for application to tropical–extratropical interactions and MJO initiation and termination.

8 Three–wave interactions

Here two types of three-wave interactions are considered as shown in figure 4:

- (1): MJO–dry baroclinic Rossby–barotropic Rossby waves (MRB)

$$\omega_{\text{MJO}}(1) + \omega_{\text{R}}(-3) + \omega_{\text{T}, Y \approx 2,000 \text{ km}}(2) = 0$$
- (2): MJO–dry Kelvin–barotropic Rossby waves (MKB)

$$\omega_{\text{MJO}}(-3) + \omega_{\text{K}}(2) + \omega_{\text{T}, Y \approx 3,000 \text{ km}}(1) = 0$$

For the acronym MRB, the M stands for MJO, the R stands for equatorial Rossby wave, and the B stands for barotropic Rossby wave; and for MKB, the M and B are the same, and the K stands for equatorial Kelvin wave. The meridional wavelength $2Y$ of the barotropic Rossby wave is chosen so that the resonance conditions (32) are exactly satisfied. The numerical results here are focused on the ODE system (24), with wave amplitudes β , α_{j_1} , and α_{j_2} , where the energy exchange between three waves is of the most interest. The coefficients in (24) for the two cases are in table 5. The RCE \bar{a} is chosen to be $\bar{a} = 0.1$ so that the small parameter $\delta = \sqrt{0.1}$.

	d_2	d_3	d_4	d_5	d_6	d_7	d_8	d_9
MRB	-0.45	-8.3e-3	-5.2e-2	1.7e-3	-0.28	-2.4e-2	1.37	0.29
MKB	0.45	-3.2e-2	-0.11	6.0e-3	0.11	7.8e-3	-8.5e-7	-7.6e-2

Table 5. Coefficients d_j for the 3-wave interaction ODEs (24) for two cases: the MJO, dry baroclinic Rossby, and barotropic Rossby wave interactions (MRB) (top row) and the MJO, dry Kelvin, and barotropic Rossby wave interactions (MKB) (bottom row).

8.1 MJO–dry baroclinic Rossby–barotropic Rossby waves (MRB)

In this case, α_{j_1} and α_{j_2} are the amplitudes for the MJO and dry baroclinic Rossby waves, respectively. To consider MJO initiation, α_{j_1} is set to be zero for the initial condition in the ODE, and the other waves have amplitudes of $|\alpha_{j_2(t=0)}| = |\beta(t=0)| = 1$. The results of the numerical simulation are shown in Figure 5. The waves exchange energy periodically, with period of about 60 days, roughly the time scale for MJO initiation and termination in nature. At early times, the MJO amplitude grows (i.e., the MJO initiates) by extracting energy from the other two waves, mainly from the dry baroclinic Rossby wave. Termination of the MJO then follows from a transfer of energy back to the dry baroclinic Rossby wave.

To explore the sensitivity of these results, different initial conditions are chosen, and the results are in figure 6. The initial amplitudes for baroclinic Rossby wave and barotropic Rossby waves are (a) $|\alpha_{j_2(t=0)}| = 0.5, |\beta(t=0)| = 1$; (b) $|\alpha_{j_2(t=0)}| = 1, |\beta(t=0)| = 0.5$; (c) $|\alpha_{j_2(t=0)}| = 0.25, |\beta(t=0)| = 1$; (d) $|\alpha_{j_2(t=0)}| = 1, |\beta(t=0)| = 0.25$. The simulations are performed with difference initial phases of α_{j_2} and β , but this has no affect on the evolution of the amplitudes. In the simulations in Figure 6, it can be seen that the amount of energy extracted by the MJO varies roughly proportionally to the amount of energy present initially in the dry baroclinic Rossby wave and barotropic Rossby wave. On the other hand, the time scale for the energy exchange changes very little among these cases. In all cases, the energy of the barotropic Rossby wave stays essentially constant and is not transferred to the MJO. These results indicate that the eventual strength of the MJO depends on the amplitude of the barotropic Rossby waves, but the MJO acquires its energy from the baroclinic rather than barotropic Rossby waves.

8.2 MJO–dry Kelvin–barotropic Rossby waves (MKB)

In this case, α_{j_1} and α_{j_2} are the amplitudes for the MJO and dry baroclinic Kelvin waves, respectively. Again considering MJO initiation, the initial conditions are $\alpha_{j_1} = 0$ and $|\alpha_{j_2(t=0)}| = |\beta(t=0)| = 1$, and the results are shown in Figure 7. While the solution is similar in character to the MRB case, two main differences can be seen. First, the temporal period of roughly 120 days is twice that of the MRB case but still within the range of time scales for MJO initiation and termination in nature. Secondly, both the dry Kelvin wave and the

barotropic Rossby waves contribute to the growth of MJO, although the energy exchange with the barotropic Rossby wave is somewhat small.

Finally, the sensitivity of the results is illustrated in Figure 8, which shows numerical results with different initial amplitudes. As in the MRB case, the amount of energy extracted by the MJO varies roughly proportionally to the amount of energy present initially in the other two modes.

9 Summary and conclusions

A new model has been proposed here to describe MJO initiation and termination and tropical-extratropical interactions. The model involves the integration of the barotropic and equatorial baroclinic modes together with moisture and convective activity envelope, all interacting together with a conserved energy. Using the method of multiscale asymptotics with multiple time scales, simplified asymptotic equations were derived for the resonant interaction of tropical and extratropical waves. The simplified model is an ODE system for wave amplitudes, including quadratic nonlinearity as in many traditional three-wave-resonance equations, and also including cubic self-interaction terms that arise from nonlinear interactions of water vapor and convective activity.

Example simulations of the ODE system are shown to illustrate some cases of MJO initiation. In this model, the MJO is shown to initiate mainly by extracting energy from either the dry Kelvin wave or the dry equatorial baroclinic Rossby wave. While the MJO extracts a smaller amount of energy from the barotropic Rossby waves, the barotropic Rossby waves are essential for MJO initiation, and the strength of the ensuing MJO depends on the strength of the barotropic Rossby waves present.

Several additional physical effects have been neglected here for simplicity. For example, the effects of climatological mean wind shear have been neglected here, although it can have a significant impact on tropical–extratropical interactions [2, 11, 27, 28, 29, 26]. It would also be interesting to include the effects of additional meridional modes that are asymmetric with respect to the equator in order to model the Boreal summer MJO and monsoon intraseasonal variability [25]. The authors are currently pursuing these issues and will report on them in the near future.

A The explicit formulation of the meridional truncated system

Applying the meridional truncation of (14) to the long-wave-scaled system of (6) leads to the **truncated system**:

$$L^2 Y B_{t'} - Y B_{x'} = \mathcal{C}_T + \delta^2 (Y B_{x'x't'} + \mathcal{D}_T) \quad (36a)$$

$$l^{(0)}_{t'} - l^{(0)}_{x'} + v^{(1)} + \frac{1}{\sqrt{2}} \delta \bar{H} a^{(0)} = \mathcal{C}_{l^{(0)}} \quad (36b)$$

$$l^{(2)}_t - l^{(2)}_x = \mathcal{C}_{l^{(2)}} \quad (36c)$$

$$r^{(0)}_{t'} + r^{(0)}_{x'} + \frac{1}{\sqrt{2}} \delta \bar{H} a^{(0)} = \mathcal{C}_{r^{(0)}} \quad (36d)$$

$$r^{(2)}_{t'} + r^{(2)}_{x'} - \sqrt{2} v^{(1)'} = \mathcal{C}_{r^{(2)}} \quad (36e)$$

$$\sqrt{2} r^{(2)} - l^{(0)} = \delta^2 (-v^{(1)'}_{t'} + \mathcal{D}_{v^{(1)}}) \quad (36f)$$

$$q^{(0)}_{t'} + \frac{\tilde{Q}}{\sqrt{2}} (r^{(0)}_{x'} - l^{(0)}_{x'}) + \frac{\tilde{Q}}{\sqrt{2}} v^{(1)'} + \delta \bar{H} a^{(0)} = \mathcal{C}_{q^{(0)}} \quad (36g)$$

$$q^{(2)}_{t'} + \frac{\tilde{Q}}{\sqrt{2}} (r^{(2)}_{x'} - l^{(2)}_{x'}) - \tilde{Q} v^{(1)'} = \mathcal{C}_{q^{(2)}} \quad (36h)$$

$$a^{(0)}_{t'} - \Gamma \bar{a} q^{(0)} = c_1 \Gamma a^{(0)} q^{(0)} + c_{10} \Gamma a^{(0)} q^{(2)} \quad (36i)$$

which is written in vector form in (19). Here \mathcal{C} and \mathcal{D} are bilinear terms at different orders:

$$\begin{aligned} \mathcal{C}_T = & -\frac{c_2}{2}(r^{(0)} - l^{(0)})_{x'}^2 - \frac{c_3}{2} \left[(r^{(0)} - l^{(0)})(r^{(2)} - l^{(2)}) \right]_{x'} \\ & - \frac{c_4}{2}(r^{(2)} - l^{(2)})_{x'}^2 - \frac{c_5}{2\sqrt{2}}(r^{(0)} - l^{(0)})v^{(1)'} - \frac{c_6}{2\sqrt{2}}(r^{(2)} - l^{(2)})v^{(1)'} \end{aligned} \quad (37a)$$

$$\begin{aligned} \mathcal{C}_{l^{(0)}} = & -c_2 B_{x'} l^{(0)} - c_8 B_{x'} l^{(2)} - 2c_2 B l^{(0)}_{x'} - c_3 B l^{(2)}_{x'} \\ & + c_2 (r^{(0)} - l^{(0)})_{B_{x'}} + \frac{c_3}{2} (r^{(2)} - l^{(2)})_{B_{x'}} - \frac{c_5}{\sqrt{2}} v^{(1)'} B \end{aligned} \quad (37b)$$

$$\begin{aligned} \mathcal{C}_{l^{(2)}} = & -c_9 B_{x'} l^{(0)} - c_4 B_{x'} l^{(2)} - c_3 B l^{(0)}_{x'} - 2c_4 B l^{(2)}_{x'} \\ & + \frac{c_3}{2} (r^{(0)} - l^{(0)})_{B_{x'}} + c_4 (r^{(2)} - l^{(2)})_{B_{x'}} - \frac{c_6}{\sqrt{2}} v^{(1)'} B \end{aligned} \quad (37c)$$

$$\begin{aligned} \mathcal{C}_{r^{(0)}} = & -c_2 B_{x'} r^{(0)} - c_8 B_{x'} r^{(2)} - 2c_2 B r^{(0)}_{x'} - c_3 B r^{(2)}_{x'} \\ & - c_2 (r^{(0)} - l^{(0)})_{B_{x'}} - \frac{c_3}{2} (r^{(2)} - l^{(2)})_{B_{x'}} + \frac{c_5}{\sqrt{2}} v^{(1)'} B \end{aligned} \quad (37d)$$

$$\begin{aligned} \mathcal{C}_{r^{(2)}} = & -c_9 B_{x'} r^{(0)} - c_4 B_{x'} r^{(2)} - c_3 B r^{(0)}_{x'} - 2c_4 B r^{(2)}_{x'} \\ & - \frac{c_3}{2} (r^{(0)} - l^{(0)})_{B_{x'}} - c_4 (r^{(2)} - l^{(2)})_{B_{x'}} + \frac{c_6}{\sqrt{2}} v^{(1)'} B \end{aligned} \quad (37e)$$

$$\mathcal{C}_{q^{(0)}} = -c_2 B_{x'} q^{(0)} - 2c_2 B q^{(0)}_{x'} - c_8 B_{x'} q^{(2)} - c_3 B q^{(2)}_{x'} \quad (37f)$$

$$\mathcal{C}_{q^{(2)}} = -c_4 B_{x'} q^{(2)} - 2c_4 B q^{(2)}_{x'} - c_9 B_{x'} q^{(0)} - c_3 B q^{(0)}_{x'} \quad (37g)$$

and

$$\mathcal{D}_T = -\frac{c_5}{\sqrt{2}L^2} \left[(r^{(0)} - l^{(0)})v^{(1)'} \right]_{x'x'} - \frac{c_6}{\sqrt{2}L^2} \left[(r^{(2)} - l^{(2)})v^{(1)'} \right]_{x'x'} + 2c_7 v^{(1)'}{}_{x'}^2 \quad (38a)$$

$$\begin{aligned} \mathcal{D}_{v^{(1)}} = & -c_7 B_{x'} v^{(1)'} - 2c_7 B v^{(1)'}_{x'} + 2c_7 v^{(1)'}_{B_{x'}} \\ & + \frac{1}{\sqrt{2}} \left[\frac{c_5}{L^2} (r^{(0)} - l^{(0)})_{B_{x'x'}} + \frac{c_6}{L^2} (r^{(2)} - l^{(2)})_{B_{x'x'}} \right] \end{aligned} \quad (38b)$$

where the coefficients c_j s are defined by parabolic cylinder functions:

$$\begin{aligned} c_1 &= \int_{-\infty}^{\infty} \Phi_0^3 dy, & c_2 &= -\frac{L}{2} \int_{-\infty}^{\infty} \Phi_0^2 \cos(Ly) dy, \\ c_3 &= -L \int_{-\infty}^{\infty} \Phi_0 \Phi_2 \cos(Ly) dy, & c_4 &= -\frac{L}{2} \int_{-\infty}^{\infty} \Phi_2^2 \cos(Ly) dy, \\ c_5 &= -L^2 \int_{-\infty}^{\infty} \Phi_0 \Phi_1 \sin(Ly) dy, & c_6 &= -L^2 \int_{-\infty}^{\infty} \Phi_1 \Phi_2 \sin(Ly) dy, \\ c_7 &= -\frac{L}{2} \int_{-\infty}^{\infty} \Phi_1^2 \cos(Ly) dy, & c_8 &= \int_{-\infty}^{\infty} \Phi_0 \Phi_2' \sin(Ly) dy, \\ c_9 &= \int_{-\infty}^{\infty} \Phi_0' \Phi_2 \sin(Ly) dy, & c_{10} &= \int_{-\infty}^{\infty} \Phi_0^2 \Phi_2 dy, \end{aligned} \quad (39)$$

Notice that the equality $c_8 + c_9 = c_3$ helps to conduct the energy conservation.

The truncated system in (36) conserves a total energy if the term $a^{(0)}q^{(2)}$ is neglected in (36i):

$$\begin{aligned} \tilde{\mathcal{E}} = & \frac{1}{4} \int_0^x 2Y L^2 (B_x^2 + B^2) + l^{(0)2} + l^{(2)2} + r^{(0)2} + r^{(2)2} + \frac{2\delta^2 \bar{H}}{\bar{Q}\Gamma} (a^{(0)} - \bar{a} \log(a^{(0)} + \bar{a})) \\ & + \frac{1}{\bar{Q}(1 - \bar{Q})} \left\{ \left[q^{(0)} - \frac{\bar{Q}}{\sqrt{2}} (r^{(0)} + l^{(0)}) \right]^2 + \left[q^{(2)} - \frac{\bar{Q}}{\sqrt{2}} (r^{(2)} + l^{(2)}) \right]^2 \right\} dx \end{aligned} \quad (40)$$

For this reason, the term $a^{(0)}q^{(2)}$ in (36i) will be neglected throughout the present paper.

B Asymptotic expansion of the truncated system

Here an explicit expansion is presented of the truncated system from (36), which was written in vector form in (19). Using an asymptotic expansion to the third order, the **ansatz** is:

$$\begin{aligned} B &= \delta^2 B_1 + \delta^3 B_2 + \delta^4 B_3 + O(\delta^5) \\ (l^{(0)}, l^{(2)}, r^{(0)}, r^{(2)}, v^{(1)'}, q^{(0)}, q^{(2)}) &= \delta^2 (l^{(0)}_1, l^{(2)}_1, r^{(0)}_1, r^{(2)}_1, v^{(1)}_1, q^{(0)}_1, q^{(2)}_1) \\ &+ \delta^3 (l^{(0)}_2, l^{(2)}_2, r^{(0)}_2, r^{(2)}_2, v^{(1)}_2, q^{(0)}_2, q^{(2)}_2) \\ &+ \delta^4 (l^{(0)}_3, l^{(2)}_3, r^{(0)}_3, r^{(2)}_3, v^{(1)}_3, q^{(0)}_3, q^{(2)}_3) + O(\delta^5) \end{aligned} \quad (41a)$$

$$a^{(0)} = \delta a^{(0)}_1 + \delta^2 a^{(0)}_2 + \delta^3 a^{(0)}_3 + O(\delta^4) \quad (41b)$$

All variables are assumed to depend on three time scales: t' and $T_1 = \delta t'$ and $T_2 = \delta^2 t'$.

To simplify notation, define $\vec{U}_n = (l^{(0)}_n, l^{(2)}_n, r^{(0)}_n, r^{(2)}_n, v^{(1)}_n, q^{(0)}_n, q^{(2)}_n, a^{(0)}_n)$, and let $\mathcal{L}_{\vec{U}}$ denote the spatial linear operator.

Using this ansatz, the truncated system (36), or its vector formulation (19), can be asymptotically expanded over three orders of magnitude. The **first order system** is

$$L^2 Y B_{1t'} - Y B_{1x'} = 0, \quad (42a)$$

$$\mathcal{N} \vec{U}_{1t'} + \mathcal{L}_{\vec{U}} \vec{U}_1 = 0, \quad (42b)$$

The **second order system** is

$$L^2 Y B_{2t'} - Y B_{2x'} = -L^2 Y B_{1T_1}, \quad (43a)$$

$$\mathcal{N} \vec{U}_{2t'} + \mathcal{L}_{\vec{U}} \vec{U}_2 = -\vec{U}_{1T_1} + \vec{F}_{\vec{U}_2}, \quad (43b)$$

The **third order system** is

$$L^2 Y B_{3t'} - Y B_{3x'} = -L^2 Y B_{1T_2} - L^2 Y B_{2T_1} + Y B_{1x'x't'} + \mathcal{C}_{1T}, \quad (44a)$$

$$\mathcal{N} \vec{U}_{3t'} + \mathcal{L}_{\vec{U}} \vec{U}_3 = -\vec{U}_{1T_2} - \vec{U}_{2T_1} + \vec{F}_{\vec{U}_3}. \quad (44b)$$

Here $\mathcal{N} = \text{diag}(1, 1, 1, 1, 0, 1, 1, 1)$ is the 8×8 matrix just to eliminate $\partial_{t'}$ for the $v^{(1)}$ variable. Forcing terms $\vec{F}_{\vec{U}_2}$ and $\vec{F}_{\vec{U}_3}$ are quantities from the lower order:

$$\vec{F}_{\vec{U}_2} = (0, 0, 0, 0, 0, 0, c_1 \Gamma a^{(0)} q^{(0)}_1), \quad (45a)$$

$$\begin{aligned} \vec{F}_{\vec{U}_3} = & (\mathcal{C}_{1l^{(0)}}, \mathcal{C}_{1l^{(2)}}, \\ & \mathcal{C}_{1r^{(0)}}, \mathcal{C}_{1r^{(2)}}, -v^{(1)}_{1t'}, \mathcal{C}_{1q^{(0)}}, \mathcal{C}_{1q^{(2)}}, c_1 \Gamma (a^{(0)} q^{(0)}_2 + a^{(0)} q^{(0)}_1)). \end{aligned} \quad (45b)$$

Here \mathcal{C}_1 denotes the bilinear operations are performed on \vec{U}_1 . Like the 2D asymptotic expansion, system (42)–(44) carries similar approximated energy conservation that

$$\frac{d}{dt'} \tilde{\mathcal{E}} = o(\delta^4). \quad (46)$$

C Details of the auxiliary problem

In this appendix, the auxiliary problem is written explicitly in terms of the new variables $\vec{W} = (K, R, Q, A, v^{(1)}, \chi)$, where the change of variables was described abstractly in section 4.

C.1 Reformulation of the auxiliary problem

Equation (21) can be concretely written as

$$\begin{cases} K_t + K_x + \frac{1}{\sqrt{2}} \bar{H} A = F_{r^{(0)}} & (47a) \end{cases}$$

$$\begin{cases} R_t + \sqrt{2} \chi_x - \sqrt{2} v^{(1)} + \bar{H} A = \sqrt{2} F_{l^{(0)}} + 2F_{r^{(2)}} & (47b) \end{cases}$$

$$\begin{cases} Q_t + \frac{\tilde{Q}}{\sqrt{2}} \left(K_x - \frac{1}{2\sqrt{2}} R_x + \frac{1}{2} \chi_x \right) + \frac{\tilde{Q}}{\sqrt{2}} v^{(1)} + \bar{H} A = F_{q^{(0)}} & (47c) \end{cases}$$

$$\begin{cases} A_t - \Gamma \bar{a} Q = F_{a^{(0)}} & (47d) \end{cases}$$

$$\begin{cases} 0 \cdot v^{(1)}_t + \chi = F_{v^{(1)}} & (47e) \\ \chi_t + \frac{1}{\sqrt{2}}R_x - 3v^{(1)} - \frac{1}{\sqrt{2}}\bar{H}A = -F_{l^{(0)}} + \sqrt{2}F_{r^{(2)}} & (47f) \end{cases}$$

$$\begin{cases} l^{(2)}_t - l^{(2)}_x = F_{l^{(2)}} & (47g) \\ q^{(2)}_t + \frac{\tilde{Q}}{\sqrt{2}}\left(\frac{1}{4}R_{x'} + \frac{\sqrt{2}}{4}\chi_{x'} - l^{(2)}_{x'}\right) - \tilde{Q}v^{(1)'} = F_{q^{(2)}} & (47h) \end{cases}$$

The equations (47e)-(47f) are used to eliminate $v^{(1)}$ and χ in the other equations:

$$\chi = F_{v^{(1)}} \quad (48a)$$

$$v^{(1)} = \frac{1}{3\sqrt{2}}(R_x - \bar{H}A) + \frac{1}{3}\left(F_{v^{(1)},t} + F_{l^{(0)}} - \sqrt{2}F_{r^{(2)}}\right) \quad (48b)$$

so that the system becomes

$$\begin{cases} K_t + K_x + \frac{1}{\sqrt{2}}\bar{H}A = F_{r^{(0)}} & (49a) \end{cases}$$

$$R_t + \frac{1}{3}R_x + \frac{4}{3}\bar{H}A = \frac{4\sqrt{2}}{3}F_{l^{(0)}} + \frac{4}{3}F_{r^{(2)}} - \sqrt{2}F_{v^{(1)},x} + \frac{\sqrt{2}}{3}F_{v^{(1)},t} \quad (49b)$$

$$\begin{cases} Q_t + \frac{\tilde{Q}}{\sqrt{2}}K_x - \frac{\tilde{Q}}{12}R_x + \left(\frac{\tilde{Q}}{6} - 1\right)\bar{H}A = \\ -\frac{\tilde{Q}}{3\sqrt{2}}F_{l^{(0)}} + \frac{\tilde{Q}}{3}F_{r^{(2)}} + F_{q^{(0)}} - \frac{\tilde{Q}}{2\sqrt{2}}F_{v^{(1)},x} - \frac{\tilde{Q}}{3\sqrt{2}}F_{v^{(1)},t} & (49c) \end{cases}$$

$$A_t - \Gamma\bar{a}Q = F_{a^{(0)}} \quad (49d)$$

$$\begin{cases} l^{(2)}_t - l^{(2)}_x = F_{l^{(2)}} & (49e) \end{cases}$$

$$\begin{cases} q^{(2)}_t - \frac{\tilde{Q}}{12\sqrt{2}}R_x - \frac{\tilde{Q}}{\sqrt{2}}l^{(2)}_x + \frac{\tilde{Q}\bar{H}}{3\sqrt{2}}A = \\ F_{q^{(2)}} + \frac{\tilde{Q}}{3}F_{l^{(0)}} - \frac{\sqrt{2}\tilde{Q}}{3}F_{r^{(2)}} - \frac{\tilde{Q}}{4}F_{v^{(1)},x} - \frac{\tilde{Q}}{3\sqrt{2}}F_{v^{(1)},t} & (49f) \end{cases}$$

When $\vec{F}_{\vec{W}} = 0$, the system (49), (49a)-(49d) forms the KRQA system as in [14], while the equation (49e) for $l^{(2)}$ is independent, and equation (49f) for $q^{(2)}$ is slaved by KRQA system and $l^{(2)}$.

C.2 Forcing vector for the auxiliary problem

Recall the earlier presentation of auxiliary problems in (42)–(44) in terms of the variables \vec{U} . In the transformation from \vec{U} to \vec{W} that was described abstractly in section 4, the forcing vector $\vec{F}_{\vec{U}}$ is transformed into forcing vector $\vec{F}_{\vec{W}}$. The

transformation of the forcing vector is now presented explicitly for each of the cases in (42)–(44). Using the notation

$$B = \delta^2 B_1 + \delta^3 B_2 + \delta^4 B_3 + O(\delta^5),$$

and

$$\vec{W} = \delta^2 \vec{W}_1 + \delta^3 \vec{W}_2 + \delta^4 \vec{W}_3 + O(\delta^5),$$

the **leading order system** is

$$L^2 Y B_{1yyt'} - Y B_{1x'} = 0 \quad (50a)$$

$$\vec{W}_{1t'} + \mathcal{L}_{\vec{W}} \vec{W}_1 = 0 \quad (50b)$$

The **second order system** is

$$L^2 Y B_{2yyt'} - Y B_{2x'} = -B_{1yyT_1}, \quad (51a)$$

$$\vec{W}_{2t'} + \mathcal{L}_{\vec{W}} \vec{W}_2 = -\vec{W}_{1T_1} + \vec{F}_{\vec{W}_2}, \quad (51b)$$

and the **third order system** is

$$L^2 Y B_{3yyt'} - Y B_{3x'} = -B_{1yyT_2} - B_{2yyT_1} + B_{1x'x't'} + \mathcal{C}_{1T} \quad (52a)$$

$$\vec{W}_{3t'} + \mathcal{L}_{\vec{W}} \vec{W}_3 = -\vec{W}_{1T_2} - \vec{W}_{2T_1} + \vec{F}_{\vec{W}_3}. \quad (52b)$$

Here

$$\vec{F}_{\vec{W}_2} = (0, 0, 0, c_1 \Gamma A_1 Q_1, 0, 0) \quad (53a)$$

$$\begin{aligned} \vec{F}_{\vec{W}_3} = & (\mathcal{C}_{1r(0)}, \frac{4\sqrt{2}}{3} \mathcal{C}_{1l(0)} + \frac{4}{3} \mathcal{C}_{1r(2)} + \sqrt{2} v^{(1)}_{1x't'} - \frac{\sqrt{2}}{3} v^{(1)}_{1t't'}, \\ & - \frac{\tilde{Q}}{3\sqrt{2}} \mathcal{C}_{1l(0)} + \frac{\tilde{Q}}{3} \mathcal{C}_{1r(2)} + \mathcal{C}_{1q(0)} + \frac{\tilde{Q}}{2\sqrt{2}} v^{(1)}_{1x't'} + \frac{\tilde{Q}}{3\sqrt{2}} v^{(1)}_{1t't'}, \\ & c_1 \Gamma (A_1 Q_2 + A_2 Q_1) + \mathcal{C}_{1a(0)}, \mathcal{C}_{1l(2)}, \\ & \mathcal{C}_{1q(2)} + \frac{\tilde{Q}}{3} \mathcal{C}_{1l(0)} - \frac{\sqrt{2}\tilde{Q}}{3} \mathcal{C}_{1r(2)} + \frac{\tilde{Q}}{4} v^{(1)}_{1x't'} + \frac{\tilde{Q}}{3\sqrt{2}} v^{(1)}_{1t't'}) \end{aligned} \quad (53b)$$

Note that for the first and second order, $\chi_1 = \chi_2 = 0$, and

$$v^{(1)}_n = \frac{1}{3\sqrt{2}} (R_{nx'} - \bar{H} A_n), \quad n = 1, 2. \quad (54)$$

D Details for multiscale analysis

D.1 Solving linear system with forcing

Here a brief summary for solving linear system with forcing is provided, which is a guideline of the multiscale analysis. Readers may find information from other

references, e.g., [10]. Let \vec{W} solve the linear system with forcing:

$$\partial_{t'} \vec{W} + \mathcal{L}_{\vec{W}} \vec{W} = \hat{F} e^{i(kx - ct')}, \vec{W}|_{t'=0} = 0. \quad (55)$$

Next, assume that \vec{W} is the superposition of eigenmodes:

$$\vec{W}(x', t') = \sum_s a_s(t') \vec{r}_s(k) e^{i(kx' - \omega_s(k)t')}. \quad (56)$$

Two cases might happen:

1. If $\omega_s(k) \neq c$, then $a_s = \frac{1}{\omega_s(k) - c} \left(e^{i(\omega_s(k) - c)t'} - 1 \right) \left(\vec{l}_s \cdot \hat{F} \right)$,
2. If $\omega_s(k) = c$, then $a_s = t \left(\vec{l}_s \cdot \hat{F} \right)$.

At the second case, when $\vec{l}_s \cdot \hat{F} \neq 0$, linear growth in time will happen. Therefore the solution \vec{W} is bounded if either 1) $\omega_s(k) \neq c$ for all s ; or 2) $\omega_s(k) = c$ and $\vec{l}_s \cdot \hat{F} = 0$. The above is the principal of the multi-scale analysis.

D.2 Solutions for the second order equations

At the second order, the only nonlinear term is in the A equation in (51). The barotropic and baroclinic modes are still decoupled. They are studied separately. For the baroclinic wave, the only nonlinear term does not generate resonance condition between different eigenmodes. Therefore, considering one mode is sufficient to study solutions for the second order equations.

Assume that the leading order solution has a form of

$$\vec{W}_1 = \alpha_{j_1} (T_1, T_2) e^{i\theta_{j_1}} \vec{r}_{j_1} + \text{C.C.}$$

Here $\theta_{j_1} = k_{j_1} x' - \omega_{j_1}(k_{j_1}) t'$ is the phase, and

$$\vec{r}_{j_1} = (\hat{K}_{1,j_1}, \hat{R}_{1,j_1}, \hat{Q}_{1,j_1}, \hat{A}_{1,j_1}, l^{(2)}_{1,j_1}, q^{(2)}_{1,j_1})$$

is the eigenvector for the $k = k_{j_1}$ eigenmode of certain wave type (e.g., Kelvin, MJO, moist Rossby, dry Rossby).

Also assume that the leading order baroclinic wind is

$$W_1 = \alpha_{j_1} e^{i\theta_{j_1}} \vec{r}_{j_1} + \alpha_{j_2} e^{i\theta_{j_2}} \vec{r}_{j_2} + \text{C.C.},$$

where $\theta_j = k_j x' + \omega_j t'$, and

$$\vec{r}_j = (\hat{K}_{1,j}, \hat{R}_{1,j}, \hat{Q}_{1,j}, \hat{A}_{1,j}, l^{(2)}_{1,j}, q^{(2)}_{1,j}), \quad j = j_1, j_2.$$

Here the eigenvectors are chosen so that $\hat{K}_{1,j}$ s are real numbers. The eigenvector \vec{r}_j are normalized by their energy unit, so that

$$E_j = \vec{r}_j^\dagger \mathcal{H} \vec{r}_j = 1, \quad j = j_1, j_2, \quad (57)$$

where \mathcal{H} is the Hessian matrix of the conserved energy for the linear system.

At the second order, the forcing terms come from the leading order (51). The solution consists of two parts: the homogeneous solution and the nonhomogeneous solution from the forcing terms. The homogeneous solution are just linear eigenmodes which is considered to be absorbed into the leading order. Therefore the second order solution is completely determined by forcing terms:

$$\vec{F} = -\alpha_{j_1} \partial_{T_1} \vec{W}_1 - \alpha_{j_1}^* \partial_{T_1} \vec{W}^* + \begin{bmatrix} 0 \\ 0 \\ 0 \\ F_3 \\ 0 \\ 0 \end{bmatrix}, \quad (58)$$

where

$$F_3 = c_1 \Gamma (\alpha_{j_1}^2 e^{i2\theta_{j_1}} \hat{A}_{1,j_1} \hat{Q}_{1,j_1} + \alpha_{j_1} \alpha_{j_1}^* \hat{A}_{1,j_1}^* \hat{Q}_{1,j_1}) + \text{C.C.}$$

The right-hand-side of the second order has three phases:

$$e^{\pm i\theta_{j_1}}, e^{\pm i2\theta_{j_1}}, \text{ and } e^0.$$

1. Phase $e^{\pm i\theta_{j_1}}$

These two phases generate secular growth. The phase $e^{i\theta_{j_1}}$ requires that

$$\vec{l}_{j_1(k_{j_1})} \cdot \hat{\vec{F}}_{(k_{j_1})} = \partial_{T_1} \alpha_{j_1} = 0.$$

The same thing applies for phase $e^{-i\theta_{j_1}}$, so that $\partial_{T_1} \alpha_{j_1} = 0$.

2. Phase $e^{\pm i2\theta_0}$

This part comes from the Q-A nonlinear term. Because it does not generate secular growth, the system can be solved and the solution is

$$\begin{aligned} \hat{W}_{2(2k_{j_1}, t', T_2)} = \\ \mathcal{R}_{(2k_{j_1})} (e^{-2i\omega_{j_1(k_{j_1})} t} \mathcal{I} - e^{-\mathcal{D}(2k_{j_1}) t}) (\mathcal{D}_{(2k_{j_1})} - 2i\omega_{j_1(k_{j_1})} \mathcal{I})^{-1} \mathcal{L}_{(2k_{j_1})} \hat{\vec{F}}_{(2k_{j_1})} \end{aligned} \quad (59)$$

3. Phase e^0

This part also stems from the Q-A nonlinear term. Although it has 0-frequencies, which may resonant with the MJO, moist Rossby mode, 0-frequency mode, fast west-propagating $l^{(2)}$ mode, but it does not happen

because

$$\vec{l}_{\text{MJO}(0)} \cdot \hat{F}_{(0)} = \vec{l}_{\text{mR}(0)} \cdot \hat{F}_{(0)} = \vec{l}_{\text{0fr}(0)} \cdot \hat{F}_{(0)} = \vec{l}_{l^{(2)}(0)} \cdot \hat{F}_{(0)} = 0,$$

which is also stated in [10]. The phase e^0 part have the contribution to the solution as

$$\hat{W}_{2(k=0,t',T_2)} = \mathcal{R}_{(0)} \left(\text{diag} \left[\begin{array}{c} \frac{1}{i\omega_{\text{K}(0)}} \\ 0 \\ 0 \\ 0 \\ \frac{1}{i\omega_{\text{R}(0)}} \\ 0 \end{array} \right] \right) (\mathcal{I} - e^{-\mathcal{D}_{(0)}t'}) \mathcal{L}_{(0)} \hat{F}_{(0)}$$

One remark is that because the leading order as forcing terms does not have T_1 dependence, the second order solution, is also independent of T_1 , i.e.,

$$\frac{\partial}{\partial T_1} \vec{W}_2 = \vec{0}.$$

D.3 Resonance condition for the third order equation

At the third order, there are nonlinear terms mixing baroclinic and barotropic terms, together with the nonlinear q - a interaction.

To simplify mathematical calculations, the \vec{W}_1 variables are transformed back to the \vec{U}_1 variables, where the Fourier coefficients can be written as

$$\begin{aligned} l^{(\hat{0})}_{1,j} &= \frac{1}{2\sqrt{2}} \hat{R}_{1,j}, & r^{(\hat{2})}_{1,j} &= \frac{1}{4} \hat{R}_{1,j}, \\ q^{(\hat{0})}_{1,j} &= \hat{Q}_{1,j}, & a^{(\hat{0})}_{1,j} &= \hat{A}_{1,j}, \\ v^{(\hat{1})}_{1,j} &= \frac{1}{3\sqrt{2}} (ik_{j1} \hat{R}_{1,j} - \bar{H} \hat{A}_{1,j}), & j &= 1, 2. \end{aligned}$$

Here the three groups of terms in (24) are explained separately:

1. Cubic terms.

The cubic terms in (24) are associated with the product of seconder order and the first order from the nonlinear q - a interaction. These terms are self-interaction – they do not interact with other eigenmodes.

Let $(K_2, R_2, Q_2, A_2, l^{(2)}_2, q^{(2)}_2)$ be the solution obtained in Section D.2. The term $c_1 \Gamma(A_1 Q_2 + A_2 Q_1)$ contributes to the resonant condition by the

nonlinear interactions between the first and second order. The leading order has phases $e^{\pm i(k_{j_1} x' - \omega_{j_1}(k_{j_1})t')}$, whereas the second order has phases $e^{\pm i(2k_{j_1} x' - 2\omega_{j_1}(k_{j_1})t')}$, $e^{\pm i(2k_{j_1} x' - \omega(2k_{j_1})t')}$, $e^{\pm i\omega_{\mathbf{K}}(0)t'}$, $e^{\pm i\omega_{\mathbf{R}}(0)t'}$, and e^0 . The product of the phases $e^{\pm i(2k_{j_1} x' - 2\omega_{j_1}(k_{j_1})t')}$ and e^0 in the second order together with the phases $e^{\pm i(k_{j_1} x' - \omega_{j_1}(k_{j_1})t')}$ at the leading order will contribute to secular growth.

The coefficient id_4 can be written as

$$d_4 = \vec{l}_{j_1} \cdot (0, 0, 0, d_{44}, 0, 0) \quad (61)$$

where

$$\begin{aligned} d_{44} = & \hat{A}_{1,j_1(-k_{j_1})} \hat{Q}_{2,j_1(2k_{j_1})} + \hat{Q}_{1,j_1(-k_{j_1})} \hat{A}_{2,j_1(2k_{j_1})} \\ & + \hat{A}_{1,j_1(k_{j_1})} \hat{Q}_{2,j_1(0)} + \hat{Q}_{1,j_1(k_{j_1})} \hat{A}_{2,j_1(0)} \end{aligned} \quad (62)$$

where \vec{l}_{j_1} is the left eigenvector of the choice of eigenmode at the leading order, and $v^{(\hat{1})}_{1,j_1}$ is in terms of \hat{R}_{1,j_1} and \hat{A}_{1,j_1} from (54), that

$$v^{(\hat{1})}_{1,j_1} = \frac{1}{3\sqrt{2}} (ik_{j_1} \hat{R}_{1,j_1} - \bar{H} \hat{A}_{1,j_1}).$$

And id_7 in the equation for α_{j_2} , same calculations are applied, but starting from another eigenmode.

2. Linear terms

Linear terms come from dispersive effect in long-wave scaled system. These are also self-interaction terms.

For the barotropic part, the coefficient for the linear term id_2 writes

$$id_2 = \frac{1}{L^2} ik_{\mathbf{T}}^2 \omega_{\mathbf{T}}.$$

For the baroclinic part, the coefficient id_5 writes

$$id_5 = \vec{l}_{j_1} \cdot (0, d_{52}, d_{53}, 0, 0, d_{56}), \quad (63)$$

where

$$d_{52} = \sqrt{2}k_{j_1}\omega_{j_1}v^{(\hat{1})}_{1,j_1} + \frac{\sqrt{2}}{3}\omega_{j_1}^2v^{(\hat{1})}_{1,j_1}, \quad (64)$$

$$d_{53} = \frac{\tilde{Q}}{2\sqrt{2}}k_{j_1}\omega_{j_1}v^{(\hat{1})}_{1,j_1} - \frac{\tilde{Q}}{3\sqrt{2}}\omega_{j_1}^2v^{(\hat{1})}_{1,j_1}, \quad (65)$$

$$d_{56} = \frac{\tilde{Q}}{4}k_{j_1}\omega_{j_1}v^{(\hat{1})}_{1,j_1} - \frac{\tilde{Q}}{3\sqrt{2}}\omega_{j_1}^2v^{(\hat{1})}_{1,j_1}. \quad (66)$$

3. Quadratic terms

The quadratic terms are associated with nonlinear baroclinic–barotropic interactions.

In (24), coefficient id_3 can be written as

$$id_3 = -\frac{1}{\sqrt{E_T}} d_{31} \quad (67)$$

where

$$\begin{aligned} d_{31} = & -i(k_{j_1} + k_{j_2})2c_2(r^{\hat{0}}_{1,j_1} - l^{\hat{0}}_{1,j_1})(r^{\hat{0}}_{1,j_2} - l^{\hat{0}}_{1,j_2}) \\ & -i(k_{j_1} + k_{j_2})2c_4(r^{\hat{2}}_{1,j_1} - l^{\hat{2}}_{1,j_1})(r^{\hat{2}}_{1,j_2} - l^{\hat{2}}_{1,j_2}) \\ & -ic_3(k_{j_1} + k_{j_2})(r^{\hat{0}}_{1,j_1} - l^{\hat{0}}_{1,j_1})(r^{\hat{2}}_{1,j_2} - l^{\hat{2}}_{1,j_2}) \\ & -ic_3(k_{j_1} + k_{j_2})(r^{\hat{0}}_{1,j_2} - l^{\hat{0}}_{1,j_2})(r^{\hat{2}}_{1,j_1} - l^{\hat{2}}_{1,j_1}) \\ & -\frac{c_5}{\sqrt{2}} \left[(r^{\hat{0}}_{1,j_1} - l^{\hat{0}}_{1,j_1})v^{\hat{1}}_{1,j_2} + (r^{\hat{0}}_{1,j_2} - l^{\hat{0}}_{1,j_2})v^{\hat{1}}_{1,j_1} \right] \\ & -\frac{c_6}{\sqrt{2}} \left[(r^{\hat{2}}_{1,j_1} - l^{\hat{2}}_{1,j_1})v^{\hat{1}}_{1,j_2} + (r^{\hat{2}}_{1,j_2} - l^{\hat{2}}_{1,j_2})v^{\hat{1}}_{1,j_1} \right] \end{aligned} \quad (68)$$

and for baroclinic mode, coefficient id_6 can be written as

$$\begin{aligned} -id_6 = & \frac{1}{\sqrt{E_T}} \vec{l}_{j_1} \cdot (\hat{F}_{r^{(0)}}_{j_2}, \frac{4\sqrt{2}}{3} \hat{F}_{l^{(0)}}_{j_2} + \frac{4}{3} \hat{F}_{r^{(2)}}_{j_2}, -\frac{\tilde{Q}}{3\sqrt{2}} \hat{F}_{l^{(0)}}_{j_2} + \frac{\tilde{Q}}{3} \hat{F}_{r^{(2)}}_{j_2} + \hat{F}_{q^{(0)}}_{j_2}, \\ & \hat{F}_{a^{(0)}}_{j_2}, \hat{F}_{l^{(2)}}_{j_2}, \frac{\tilde{Q}}{3} \hat{F}_{l^{(0)}}_{j_2} - \frac{\sqrt{2}\tilde{Q}}{3} \hat{F}_{r^{(2)}}_{j_2} + \hat{F}_{q^{(2)}}_{j_2}), \end{aligned} \quad (69)$$

where \vec{l}_{j_1} is the left eigenvector for the j_1 baroclinic mode, and \hat{F} are Fourier coefficients of interactions between j_2 baroclinic mode and barotropic wind. They corresponds to bilinear terms \mathcal{C} s in (37). One example is given for $\hat{F}_{l^{(0)}}_{j_2}$:

$$\begin{aligned} \hat{F}_{l^{(0)}}_{j_2} = & -ik_T \left(c_2 l^{\hat{0}}_{1,j_2} + c_8 l^{\hat{2}}_{1,j_2} \right) - ik_{j_2} \left(2c_2 l^{\hat{0}}_{1,j_2} + c_3 l^{\hat{2}}_{1,j_2} \right) \\ & + ik_T \left[c_2 (r^{\hat{0}}_{1,j_2} - l^{\hat{0}}_{1,j_2}) + \frac{c_3}{2} (r^{\hat{2}}_{1,j_2} - l^{\hat{2}}_{1,j_2}) \right] - \frac{c_5}{\sqrt{2}} v^{\hat{1}}_{1,j_2} \end{aligned} \quad (70)$$

The coefficient d_9 is analogous to d_6 by swapping j_1 and j_2 .

Acknowledgment: The research of A.J.M. is partially supported by Office of Naval Research grant ONR MURI N00014-12-1-0912. The research of S.N.S. is

partially supported by Office of Naval Research grant ONR MURI N00014-12-1-0912, ONR Young Investigator Award ONR N00014-12-1-0744, and National Science Foundation grant NSF DMS-1209409. S.C. is supported as a postdoctoral research associate by the ONR grants.

References

- [1] A. D. D. Craik. *Wave Interactions and Fluid Flows*. Cambridge Univ Press, Cambridge, 1985.
- [2] B. J. Hoskins and F.-F. Jin. The initial value problem for tropical perturbations to a baroclinic atmosphere. *Q. J. R. Meteorol. Soc.*, 117:299–317, 1991.
- [3] F.-F. Jin and B. J. Hoskins. The direct response to tropical heating in a baroclinic atmosphere. *J. Atmos. Sci.*, 52(3):307–319, February 1995.
- [4] B. Khouider and A. J. Majda. A non-oscillatory balanced scheme for an idealized tropical climate model: Part I: Algorithm and validation. *Theor. Comp. Fluid Dyn.*, 19(5):331–354, 2005.
- [5] G. N. Kiladis, M. C. Wheeler, P. T. Haertel, K. H. Straub, and P. E. Roundy. Convectively coupled equatorial waves. *Rev. Geophys.*, 47:RG2003, 2009.
- [6] W. K. M. Lau and D. E. Waliser, editors. *Intraseasonal Variability in the Atmosphere–Ocean Climate System*. Springer, Berlin, 2012.
- [7] R. A. Madden and P. R. Julian. Detection of a 40–50 day oscillation in the zonal wind in the tropical Pacific. *J. Atmos. Sci.*, 28(5):702–708, 1971.
- [8] R. A. Madden and P. R. Julian. Description of global-scale circulation cells in the Tropics with a 40–50 day period. *J. Atmos. Sci.*, 29:1109–1123, September 1972.
- [9] R. A. Madden and P. R. Julian. Observations of the 40–50-day tropical oscillation—a review. *Mon. Wea. Rev.*, 122:814–837, 1994.
- [10] A. J. Majda. *Introduction to PDEs and Waves for the Atmosphere and Ocean*, volume 9 of *Courant Lecture Notes in Mathematics*. American Mathematical Society, Providence, 2003.
- [11] A. J. Majda and J. A. Biello. The nonlinear interaction of barotropic and equatorial baroclinic Rossby waves. *J. Atmos. Sci.*, 60:1809–1821, August 2003.
- [12] A. J. Majda and M. G. Shefter. Models of stratiform instability and convectively coupled waves. *J. Atmos. Sci.*, 58:1567–1584, 2001.
- [13] A. J. Majda and S. N. Stechmann. A simple dynamical model with features of convective momentum transport. *J. Atmos. Sci.*, 66:373–392, 2009.
- [14] A. J. Majda and S. N. Stechmann. The skeleton of tropical intraseasonal oscillations. *Proc. Natl. Acad. Sci. USA*, 106(21):8417–8422, 2009.
- [15] A. J. Majda and S. N. Stechmann. Nonlinear dynamics and regional variations in the MJO skeleton. *J. Atmos. Sci.*, 68:3053–3071, 2011.
- [16] A. Matthews, B. J. Hoskins, and M. Masutani. The global response to tropical heating in the madden-julian oscillation during the northern winter. *Q. J. R. Meteorol. Soc.*, 130:1991–2011, 2004.



- [17] A. Matthews and G. N. Kiladis. The tropical-extratropical interaction between high-frequency transients and the madden-julain oscillation. *Mon. Wea. Rev.*, 127:661–677, May 1999.
- [18] J. David Neelin and Ning Zeng. A quasi-equilibrium tropical circulation model—formulation. *J. Atmos. Sci.*, 57:1741–1766, 2000.
- [19] J. Pedlosky. *Geophysical Fluid Dynamics*. Springer–Verlag, 2nd edition, 1987.
- [20] P. Ray and C. Zhang. A case study of the mechanics of extratropical influence on the initiation of the Madden-Julian oscillation. *J. Atmos. Sci.*, 67, February 2010.
- [21] P. Ripa. On the theory of nonlinear wave-wave interactions among geophysical waves. *J. Fluid Mech.*, 103:87–115, 1981.
- [22] P. Ripa. Nonlinear wave-wave interactions in a one-layer reduced-gravity model on the equatorial β plane. *J. Phys. Ocean.*, 12(1):97–111, 1982.
- [23] J. P. Stachnik, D. E. Waliser, and A. J. Majda. Precursor environmental conditions associated with the termination of Madden–Julian oscillation events. *J. Atmos. Sci.*, 72(5):1908–1931, 2015.
- [24] S. N. Stechmann and A. J. Majda. Identifying the skeleton of the Madden–Julian oscillation in observational data. *Mon. Wea. Rev.*, 143:395–416, 2015.
- [25] S. Thual, A. J. Majda, and S. N. Stechmann. Asymmetric intraseasonal events in the stochastic skeleton MJO model with seasonal cycle. *Climate Dynamics*, page in press, 2015.
- [26] B. Wang and X. Xie. Low-frequency equatorial waves in vertically sheared zonal flow. part i: Stable waves. *J. Atmos. Sci.*, 53:449–467, 1996.
- [27] P. J. Webster. Reponse of the tropical atmosphere to local, steady forcing. *Mon. Wea. Rev.*, 10(7):518–541, July 1972.
- [28] P. J. Webster. Mechanisms determining the atmospheric response to sea surface temperature anomalies. *J. Atmos. Sci.*, 38:554–571, 1981.
- [29] P. J. Webster. Seasonality in the local and remote atmospheric response to sea surface temperature anomalies. *J. Atmos. Sci.*, 39:41–52, 1982.
- [30] K. M. Weickmann. Intraseasonal circulation and outgoing longwave radiation modes during northern hemisphere winter. *Mon. Wea. Rev.*, 111:1838–1858, September 1983.
- [31] K. M. Weickmann and E. Berry. The tropical madden-julian oscillation and the global wind oscillation. *Mon. Wea. Rev.*, 137:1601–1614, May 2009.
- [32] K. M. Weickmann, G. R. Lussky, and Kutzback J. E. Intraseasonal (30-60 day) fluctuations of outgoing longwave radiation and 250 mb streamfunction during northern winter. *Mon. Wea. Rev.*, 113:941–961, June 1985.
- [33] C. Zhang. Madden–Julian Oscillation. *Reviews of Geophysics*, 43:RG2003, June 2005.

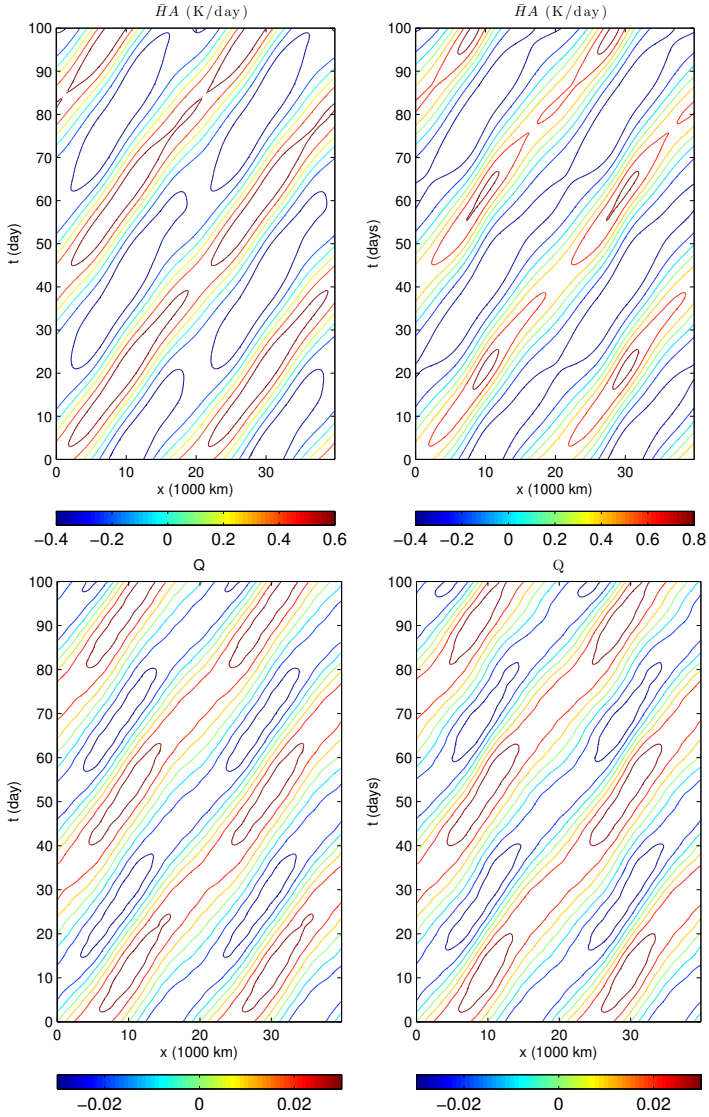


Fig. 2. Comparisons between asymptotic solutions (left) and numerical ('true') solutions (right) for $\bar{A} = 0.1$ for the case of a wavenumber-2 MJO mode. The convective activity $\bar{H}A$ (top) and the water vapor Q (bottom) are shown as functions of x and t .

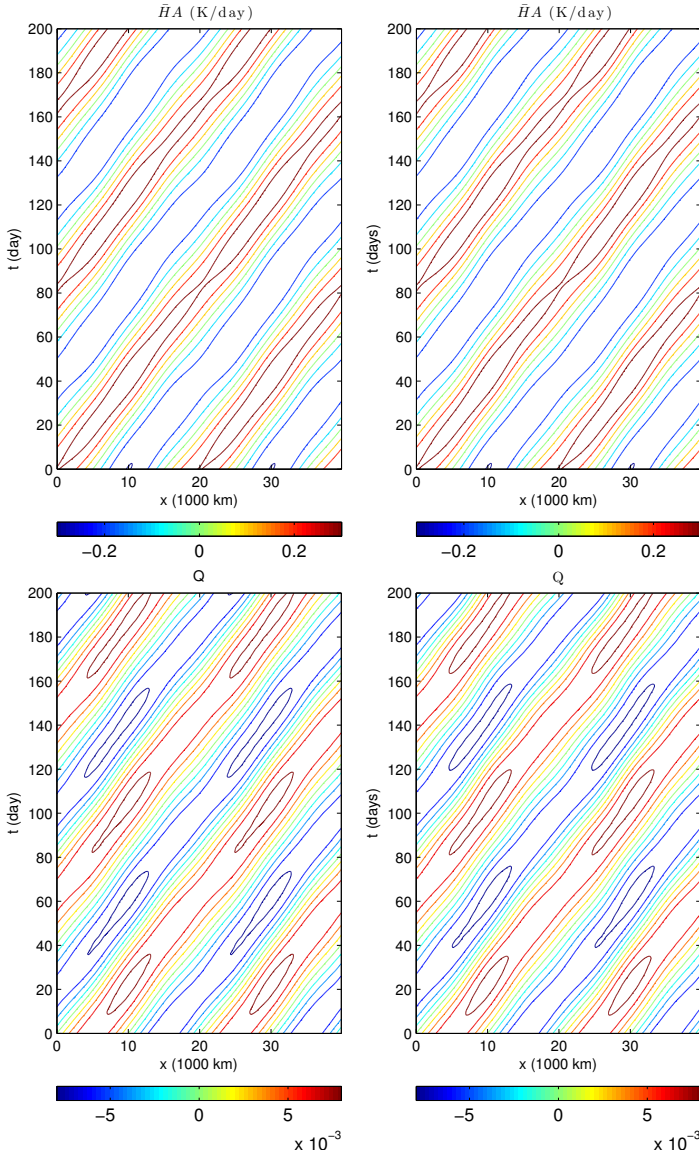


Fig. 3. Comparisons between asymptotic solutions (left) and numerical ('true') solutions (right) for $\bar{A} = 0.025$ for the case of a wavenumber-2 MJO mode. The convective activity $\bar{H}A$ (top) and the water vapor Q (bottom) are shown as functions of x and t .

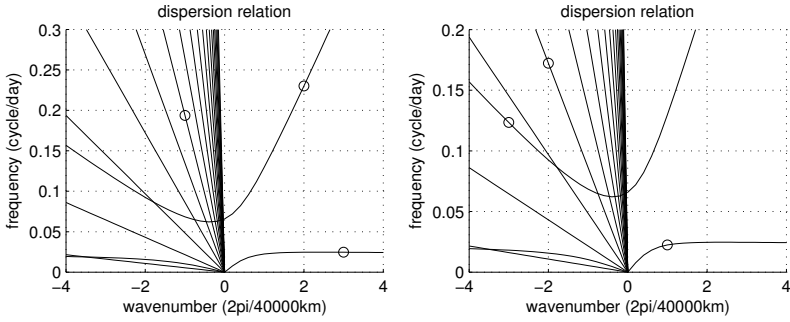


Fig. 4. Resonance condition for three-wave interactions, where circles indicate the particular wave numbers and frequencies that leads to resonances. Left: MJO, Kelvin and barotropic Rossby wave; right: MJO, Rossby and barotropic Rossby wave.

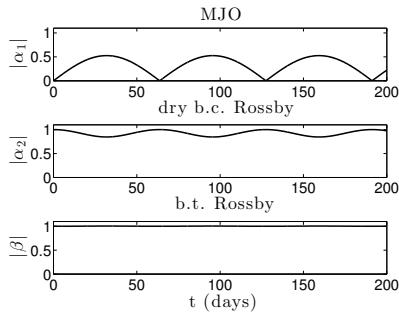


Fig. 5. MJO–Rossby–barotropic Rossby wave interactions. Initial condition: $\alpha_{j_1} = 0$, $|\alpha_{j_2}(t=0)| = |\beta(t=0)| = 1$.

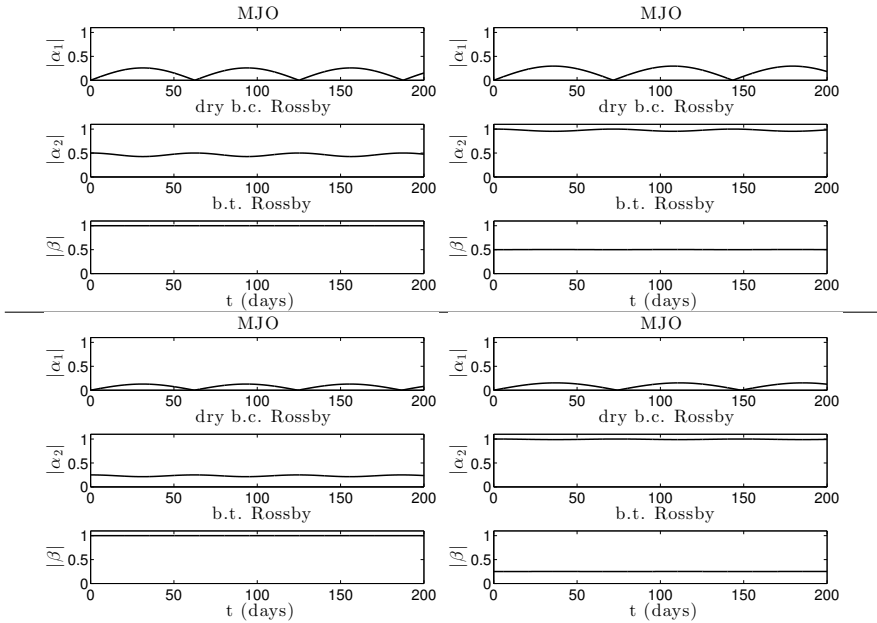


Fig. 6. MJO–Rossby–barotropic Rossby wave interactions. Initial condition: $\alpha_{j_1} = 0$. (a) $|\alpha_{j_2(t=0)}| = 0.5, |\beta_{(t=0)}| = 1$; (b) $|\alpha_{j_2(t=0)}| = 1, |\beta_{(t=0)}| = 0.5$; (c) $|\alpha_{j_2(t=0)}| = 0.25, |\beta_{(t=0)}| = 1$; (d) $|\alpha_{j_2(t=0)}| = 1, |\beta_{(t=0)}| = 0.25$.

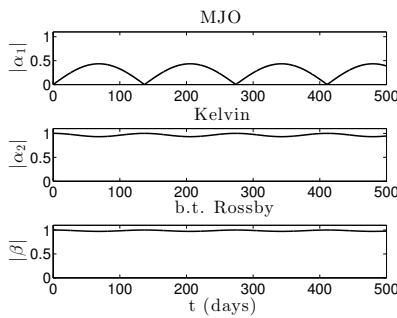


Fig. 7. MJO–Kelvin–barotropic Rossby wave interactions. Initial condition: $\alpha_{j_1} = 0, |\alpha_{j_2(t=0)}| = |\beta_{(t=0)}| = 1$.

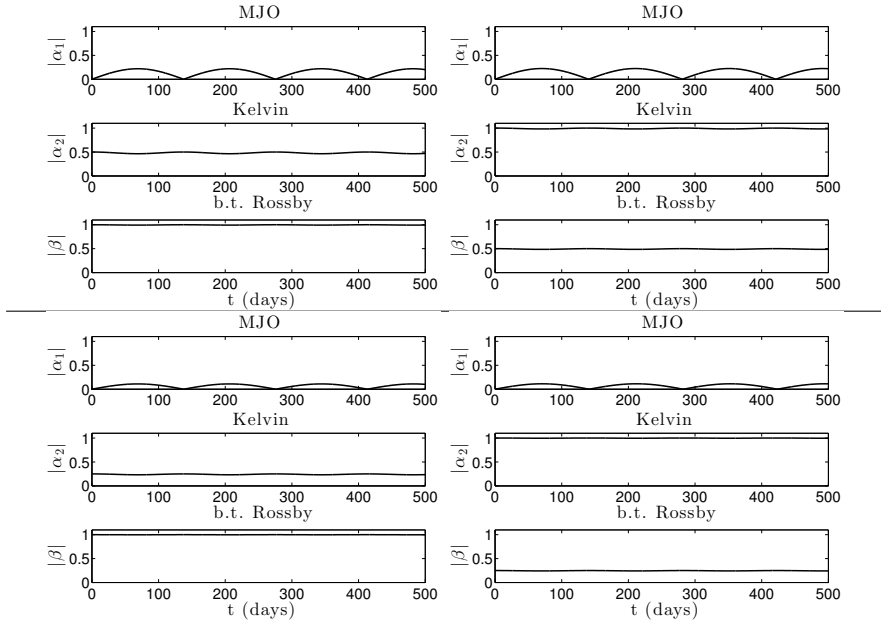


Fig. 8. MJO–Kelvin–barotropic Rossby wave interactions. Initial condition: $\alpha_{j_1} = 0$. (a) $|\alpha_{j_2}(t=0)| = 0.5, |\beta(t=0)| = 1$; (b) $|\alpha_{j_2}(t=0)| = 1, |\beta(t=0)| = 0.5$; (c) $|\alpha_{j_2}(t=0)| = 0.25, |\beta(t=0)| = 1$; (d) $|\alpha_{j_2}(t=0)| = 1, |\beta(t=0)| = 0.25$.